



HAL
open science

Lithological controls on lake water biogeochemistry in Maritime Antarctica

Nazlı Olgun, Ufuk Tari, Nurgül Balcı, Şafak Altunkaynak, Işıl Gürarşlan,
Sevil Deniz Yakan, Frederic Thalasso, María Soledad Astorga-España, Léa
Cabrol, Céline Lavergne, et al.

► **To cite this version:**

Nazlı Olgun, Ufuk Tari, Nurgül Balcı, Şafak Altunkaynak, Işıl Gürarşlan, et al.. Lithological controls on lake water biogeochemistry in Maritime Antarctica. *Science of the Total Environment*, 2023, 912, 10.1016/j.scitotenv.2023.168562 . hal-04453934

HAL Id: hal-04453934

<https://hal.science/hal-04453934>

Submitted on 17 Apr 2024

HAL is a multi-disciplinary open access archive for the deposit and dissemination of scientific research documents, whether they are published or not. The documents may come from teaching and research institutions in France or abroad, or from public or private research centers.

L'archive ouverte pluridisciplinaire **HAL**, est destinée au dépôt et à la diffusion de documents scientifiques de niveau recherche, publiés ou non, émanant des établissements d'enseignement et de recherche français ou étrangers, des laboratoires publics ou privés.

Lithological controls on lake water biogeochemistry in Maritime Antarctica

Nazlı Olgun^{a,*}, Ufuk Tari^b, Nurgül Balcı^c, Şafak Altunkaynak^b, Işıl Gürarslan^b,
Sevil Deniz Yakan^d, Frederic Thalasso^{e,1}, María Soledad Astorga-España^f, Léa Cabrol^{g,2},
Céline Lavergne^h, Linn Hoffmannⁱ

^a Eurasia Institute of Earth Sciences, Istanbul Technical University (ITU), 34469 Maslak, Istanbul, Turkey

^b Faculty of Mines, Department of Geological Engineering, Istanbul Technical University (ITU), 34469 Maslak, Istanbul, Turkey

^c Biogeochemistry Laboratory, Department of Geological Engineering, Istanbul Technical University, Istanbul, Turkey

^d Faculty of Naval Architecture and Ocean Engineering, Istanbul Technical University (ITU), 34469 Maslak, Istanbul, Turkey

^e Centro de Investigación y de Estudios Avanzados del IPN (Cinvestav), Depto. Biotecnología y Bioingeniería, Av. IPN. 2508, San Pedro Zacatenco C.P. 07360, Mexico

^f Environmental Biogeochemistry Laboratory (EBL), University of Magallanes, Punta Arenas, Chile

^g Aix-Marseille University, Mediterranean Institute of Oceanography (M.I.O, UMR 110), CNRS, IRD, Marseille, France

^h HUB Ambiental UPLA and Laboratory of Aquatic Environmental Research (LACER), Universidad de Playa Ancha, Subida Leopoldo Carvallo 207, Valparaíso 234000, Chile

ⁱ Department of Botany, University of Otago, PO Box 56, Dunedin 9016, New Zealand

Science of the Total Environment 912 (2024) 168562

* Corresponding author.

E-mail address: nokiyak@itu.edu.tr (N. Olgun).

¹ Cape Horn International Center, Universidad de Magallanes, Punta Arenas, Chile.

² Millennium Institute Biodiversity of Antarctic and Subantarctic Ecosystems (BASE), Santiago, Chile.

<https://doi.org/10.1016/j.scitotenv.2023.168562>

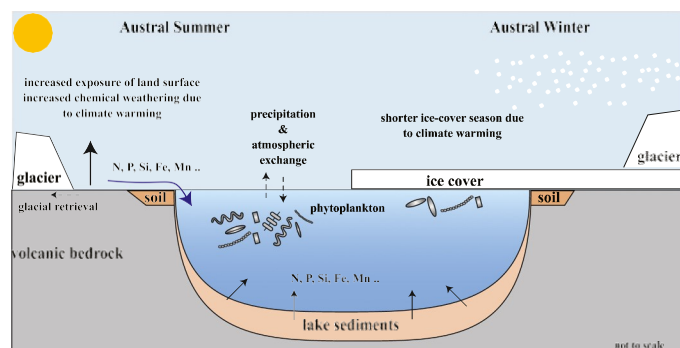
Received 24 July 2023; Received in revised form 4 November 2023; Accepted 11 November 2023

Available online 18 November 2023

HIGHLIGHTS

- Biogeochemical properties of lakes, ponds and one stream in Maritime Antarctica were characterized.
- Significant differences in terms of phytoplankton populations were observed in the Fildes Peninsula and Ardley Islands
- P-limitation is very likely in lakes in King George Island
- Input of N, P, Si and Fe from sediments, soils and rocks were shown by the leaching experiments.
- Climate warming can increase in input of bio-relevant elements from the lithology into the lakes

GRAPHICAL ABSTRACT



Editor: Jay Gan

Keywords:

Antarctica

King George Island

Phytoplankton

Lake

Lithology

Leaching

Nutrients

ABSTRACT

Although the Antarctic lakes are of great importance for the climate and the carbon cycle, the lithological influences on the input of elements that are necessary for phytoplankton in lakes have so far been insufficiently investigated. To address this issue, we analyzed phytoplankton cell concentrations and chemical compositions of water samples from lakes, ponds and a stream on Fildes and Ardley Islands of King George Island in the South Shetland Archipelago. Furthermore, lake sediments, as well as soil and rock samples collected from the littoral zone were analyzed for their mineralogical/petrographic composition and pollutant contents of polycyclic aromatic hydrocarbons (PAHs). In addition, leaching experiments were carried out to investigate the possible changes in pH, alkalinity, macronutrients (N, P, Si), micronutrients (e.g. Fe, Zn, Cu, Mn), anions (S, F, Br), and other cations (e.g. Na, K, Mg, Ca, Al, Ti, V, Cr, Co, Ni, As, Se, Pb, Sb, Mo, Ag, Cd, Sn, Ba, Tl, B). Our results showed that phytoplankton levels varied between 15 and 206 cells/mL. Chlorophyll-a concentrations showed high correlations with NH_4 , NO_3 . The low levels of PO_4 (<0.001 mg/L) indicated a possible P-limitation in the studied lakes. The composition of rock samples ranged from basalt to trachybasalt with variable major oxide (e.g. SiO_2 , Na_2O and K_2O) contents and consist mainly quartz, albite, calcite, dolomite and zeolite minerals. The concentrations of total PAHs were below the toxic threshold levels ($9.55\text{--}131.25$ ng g^{-1} dw). Leaching experiments with lithologic samples indicated major increase in pH (up to 9.77 ± 0.02) and nutrients, especially PO_4 (1.03 ± 0.04 mg/L), indicating a strong P-fertilization impact in increased melting scenarios. Whereas, toxic elements such as Pb, Cu, Cd, Al and As were also released from the lithology, which may reduce the phytoplankton growth.

1. Introduction

Antarctica is a unique environment with the coldest and driest climate on Earth. The prospects for the future of Antarctica indicate that more and more new land areas will be exposed due to the melting, thinning and retreat of glaciers (Rintoul et al., 2018). Annual mean temperatures in West Antarctica and Antarctic Peninsula region have increased by around 3 °C since the 1950s and 87 % of the glaciers began to retreat due to melting (Kunz et al., 2012; Schofield et al., 2010; Turner et al., 2005). As a result of increased ice melting, Antarctic freshwater systems experience rapid expansion and change in their biogeochemistry.

The primary productivity of lakes in particular can play a critical role in climate relevant gases such as carbon dioxide (CO₂) and methane (CH₄) into the atmosphere (West et al., 2015). It is estimated that around 6–16 % of natural global methane (CH₄) comes from the lakes (Bastviken et al., 2004; Borrel et al., 2011). The marine lakes on King George Island, on the other hand, are dominated by autotrophs and serve as a sink for atmospheric carbon dioxide (Thalasso et al., 2022). Chlorophyll- a (chl-a), the pigment produced by phytoplankton, is often used as an indicator of aquatic primary productivity. The Chl-a concentration in the lakes of the maritime Antarctic quadrupled between 1980 and 1996 on Signy Island (Qayle et al., 2002). On the contrary, phytoplankton deficiency in lakes of the McMurdo Dry Valley was reported previously (Priscu, 1995). However, the reasons for the remarkable changes in phytoplankton production in Antarctic lakes are not yet fully understood. Which geochemical parameters influence the phytoplankton levels in Antarctic marine lakes? Can nutrients and other elements related to lithology play an important role compared to faunal, atmospheric and anthropogenic sources in the region?

The lithology of Antarctica consists mainly of volcanic rocks (Birkenmajer and Zastawniak, 1989; Gao et al., 2018; Hawkes, 1961; Machado et al., 2005). Exposed lithology dominated by volcanic rocks is susceptible to chemical weathering, which can affect water chemistry in catchments. Melt waters and rainwaters that interact with rocks and soils profoundly impact the elemental composition of the inflow water to the lakes (Raiswell, 1984). Lake sediments can also interact with the lake waters via re-suspension and leaching, thus providing bio-relevant elements like nutrients (N, P, Si) and other metals such as Fe, Mg, and Mn (El Bilali et al., 2002).

The inflow of river water is one of the main factors influencing the geochemistry of the lake during the ice-free period in the region (Alfonso et al., 2015; Malandrino et al., 2009), and to a lesser extent atmospheric input (Préndez and Carrasco, 2003). In addition, the local fauna also plays a role in ornithogenic soil formation under the influence of birds in the form of guano, feathers, and eggshells in the Antarctic (Emslie et al., 2014). Moreover, the soil structure is also affected by the sea-salt aerosols and therefore characterized as salty soil (Hall et al., 1993).

In this study, we analyzed the biogeochemical parameters of six lakes, five ponds and one stream on the Fildes and Ardley Islands of King George Island, in the South Shetland Archipelago, located 120 km off the coast of the Antarctic Peninsula. Lithological samples, consisting of lake sediments, soil and rock samples, were examined for elemental, mineralogical/petrographic composition and leaching behavior. Possible pollution was investigated on the basis of the content of poly-cyclic aromatic hydrocarbons (PAHs) and heavy metals (As, Mo, Ag, Cd, Sn, Sb, Ba, Tl, B, Pb, Zn and Cu).

2. Study region, samples, and methods

2.1. Study region

The study area is located on King George Island (62°02' S, 58°21' W), the northernmost of the South Shetland Islands in Maritime Antarctica (Fig. 1). King George Island is about 95 km long, 25 km wide and has an area of 1150 km², 92 % of which is covered by Collins Glacier (Fig. 1). Ardley Island is connected to the Fildes Peninsula at low tide by an approximately 30 m long sand barrier that allows passage between the Fildes Peninsula and Ardley Island. Ardley Island is an Antarctic Sanctuary (ASP 150) with important colonies of gentoo penguins, Adela penguins and chinstrap penguins. The vegetation in the study region consists only of lichens and mosses (Yogui and Sericano, 2008). The annual number of freeze-thaw cycles on the Fildes Peninsula is 120 to 122 (Schmid et al., 2017). The meltwater from snow, ice, and glaciers influences the hydrological system in the study region. The study region is also one of the most populated regions in Antarctica as Fildes Peninsula hosts five scientific research bases and Ardley Island hosts one shelter-type station (Fig. 1).

The land surface area of Fildes and Ardley mainly consists of volcanic rocks consisting of lavas, dikes, and associated pyroclastic rocks along with the shoreface deposits (Fig. 1). Fildes Peninsula lithology is composed of basalt, basalt-andesitic lavas, volcanic breccia, agglomerate, conglomerate and volcanic tuff deposits (Fig. 1). Ardley Island is mainly covered with pyroclastic rocks of fragmented basaltic andesite, andesitic lava along with volcanic breccia, tuff, and fossil intercalated volcanic sediments (Fig. 1). The geology and paleoclimatology of the King George Island were described previously (Birkenmajer and Zastawniak, 1989; Gao et al., 2018; Hawkes, 1961; Machado et al., 2005). The ages of the volcanic rocks in the study region have been determined as late Paleocene (59 Ma) – Middle Eocene (43–42 Ma) (Fensterseifer et al., 1988; Pankhurst and Smellie, 1983; Smellie et al., 1984; Soliani et al., 1988).

2.2. Sampling strategy

Six lakes, five ponds and one stream on the Fildes Peninsula and Ardley Island on King George Island were surveyed (Table 1). Water, sediment, soil and rock samples were collected to assess the potential effects of the surrounding lithology on the biogeochemistry of the lakes. Samples were collected during fieldwork between February 12 and March 7, 2017 (Fig. 2). All research activities were conducted in careful compliance with the environmental guidelines for field research in Antarctica established by the Scientific Committee on Antarctic Research (SCAR). Permits for sampling and sample transportation were granted by the Instituto Antarctica Chileno (INACH).

Water samples: The bottles used for water sampling in the field were

Table 1 Geographic information of the studied lakes located in Fildes and Ardley Peninsulas in King George Island, Antarctic. The field studies were performed on 17 February–7 March 2017. The smaller water bodies were named Pond (P), ponds with high organic activity were named Organic Pond (OP), and the stream hereafter Babylon Stream (Bab.).

Lake1 Lake2 Bab. (stream) Lake3 Lake4 Lake5 Lake6 Pond1 Pond2 Pond3 OP1 OP2	Peninsula	Other names	Area (m ²)	Latitude	Longitude	Distance from		Altitude (m)	Literature
						shore (m)	glacier (m)		
	Fildes	Uruguay, Glubokoye, Glubokoe	70,933.0	-62.1853	-58.9118	138	542	25	(Alfonso et al., 2015; Thalasso et al., 2022)
	Fildes	Kitiesh, Kitezsh, Kitesch	93,527.2	-62.1936	-58.9664	587	3160	15	(Alfonso et al., 2015; Perendez and Carrasco, 2003; Thalasso et al., 2022)
	Fildes	-	-	-62.194033	-58.961448	761	3240	-	-
	Fildes	-	6417.1	-62.2010	-58.9729	763	4020	40	(Préndez and Carrasco, 2003; Thalasso et al., 2022)
	Fildes	Langer, Dlimmoye	23,001.0	-62.2050	-58.9665	312	3910	15	(Thalasso et al., 2022)
	Fildes	West, Gran Muralla Lake, Xihou Lake	11,888.3	-62.2172	-58.9660	250	5060	18	(Alfonso et al., 2015; Perendez and Carrasco, 2003; Thalasso et al., 2022)
	Fildes	-	4508.2	-62.2210	-58.9590	270	5260	15	(Thalasso et al., 2022)
	Fildes	-	3272.4	-62.1893	-58.9295	616	1510	60	(Thalasso et al., 2022)
	Fildes	-	2804.9	-62.1920	-58.9417	373	2110	25	(Thalasso et al., 2022)
	Fildes	-	2451.9	-62.1944	-58.9486	370	2580	35	(Thalasso et al., 2022)
	Fildes	-	385.4	-62.1887	-58.9242	359	1250	45	(Thalasso et al., 2022)
	Ardley	-	872.0	-62.2104	-58.9410	145	3760	24	(Thalasso et al., 2022)

cleaned with acid, rinsed with distilled water in the laboratory and rinsed three times with the sample water before sampling in the field. The water samples were then filled into sterile plastic containers and stored in the Escudero base in a dark and cool place. The water samples for the composition of dissolved anions and cations were filtered through polycarbonate filters with a pore size of 0.45 µm (Millipore®). For the cation analyses, nitric acid was added to the water samples to reduce the pH value below 2 (pH < 2, 1 µL 15 % HNO₃ per mL sample).

Sediment, soil and rock samples: The lake sediment sample from the center of Lake Kitiesh (L2) was collected from the lake bottom using an Ekman dredge, while the other lake sediments, soils and rocks were collected from the littoral zone of the lakes. For PAH analyses, a small portion (2–5 g) of selected sediment and soil samples from the Kitiesh Lake region (L2) in Fildes and OP2 in Ardley Island were wrapped in aluminum foil and stored in the ultra-freezers. The rock samples were collected by hand from the outcropping volcanic rocks or from the littoral zone of the investigated lakes (Fig. 1). A rock sample from the Flat Top peninsula, located southwest of the Fildes, was also collected (Fig. 1). Depending on the analysis, selected rock samples were used for petrographic, mineralogical and elemental analyses and for determining the composition of the lava (Supplementary Table S1).

2.3. Phytoplankton cell count

For the analysis of phytoplankton cells, the water samples were treated with Merck® Lugol's iodine solution (containing potassium iodide and iodine) for preservation and then coated with aluminum foil to avoid sunlight. The water samples were stored in a dark and cool place until analysis. Phytoplankton cell counting was carried out using surface water samples from Kitiesh Lake (L2) and OP2. The water sample from Kitiesh Lake was taken from the center of the lake, while the water sample from OP2 was taken from the shore. For the cell count determination of phytoplankton, the water samples were concentrated by sedimentation of 5 L water sample and back-suction method. The phytoplankton species were counted according to Utermöhl (1958) using an Accu-Scope inverted microscope (Olympus) (Utermöhl, 1958).

2.4. Lake water ion concentration analyses

Lake water of dissolved nutrients NH₄⁺, NO₂⁻, NO₃⁻, PO₄³⁻ and volatiles SO₄²⁻, Cl⁻, F⁻, Br⁻ were measured by ion chromatography (DIONEX Model: 3000 DUAL ICS). The concentrations of dissolved metals and other cations Na⁺, K⁺, Mg²⁺, Ca²⁺, Al³⁺, Si⁴⁺, P³⁺, Ti⁴⁺, V⁵⁺, Cr⁶⁺, Mn⁴⁺, Fe³⁺, Co²⁺, Ni²⁺, Cu²⁺, Zn²⁺, As³⁺, Se⁶⁺, Pb²⁺, Sb⁵⁺, Mo⁶⁺, Ag⁺, Cd²⁺, Sn²⁺, Ba²⁺, Tl³⁺ and B³⁺ were measured by Inductively Coupled Plasma - Mass Spectrometer (ICP-MS) following the TS EN ISO 17294-2 method by using an Agilent 7500ce ICP-MS. Spectrally pure Argon gas (99.998) was used with a flow rate of 15 L min⁻¹. The standards and the diluted samples were prepared using ultra-pure water with 18 MΩ/cm. Repeat measurements were performed in every ten samples. External calibrations were done for each sample and Li, Sc, Ge, In, and Bi elements were used for internal calibrations. The detection limits of elements in ICP-MS analyses were 0.001 mg/L.

Physicochemical parameters including lake water pH, temperature, conductivity, total dissolved solids (TDS), and salinities were measured in the field by a Hanna HI 9828 portable multi-parameter probe (Thalasso et al., 2022). Alkalinities were determined from carbonate and bicarbonate concentrations that were measured by titration method. Lake water chl-a concentrations were determined spectrophotometrically by 95 % acetone filter pigment extraction method, using a Shimadzu UV Mini 1240 spectrophotometer at the Chilean Escudero Base described previously in Thalasso et al., 2022 (Table 2).

2.5. Mineralogy, petrography, and element concentration analyses

The mineralogical composition of seven pulverized samples (Kit-Sed,

Table 2

Physicochemical properties, chlorophyll-a concentrations, phytoplankton cell count, alkalinity, nutrients, and other elements of the lakes, streams, and ponds. ¹Dis. O₂, dissolved oxygen, Cond., conductivity, TDS, total dissolved solids, and chl-a data were presented in [Thalasso et al., 2022](#), except for the Babylon stream. Detection limits were 0.001 mg/L for IC and ICP-MS analyses.

	L1 (Uruguay)	L2 (Kitiesh)	Bab.	L3	L4 (Langer)	L5 (West)	L6	P1	P2	P3	OP1	OP2
pH ¹	7.40	7.23	-	8.50	8.03	7.82	7.95	8.80	9.18	8.44	8.56	8.48
Dis. O ₂	87.5 %	88.7 %	-	97.0 %	89.7 %	84.1 %	97.4 %	100.0 %	100.0 %	93.1 %	98.1 %	100.0 %
Temp. (°C) ¹	5.25	2.52	-	0.88	1.74	2.01	1.51	5.51	3.28	5.21	5.14	0.97
Cond. (µS/cm) ¹	95	208	-	115	206	75	111	68	37	100	57	256
Salinity (PSU) ¹	0.04	0.10	-	0.05	0.10	0.03	0.05	0.03	0.02	0.05	0.03	0.12
TDS (mg/L) ¹	48	104	-	58	103	38	56	34	18	50	28	128
Chl-a (µg/L) ¹	0.29	1.35	-	0.31	0.35	0.50	1.46	0.77	0.50	0.79	2.64	6.92
Phytoplankton (cells mL ⁻¹)	-	15	-	-	-	-	-	-	-	-	-	206
CO ₃ ²⁻ (mg/L) ¹	0.00	0.00	-	0.00	0.00	0.00	0.00	0.00	0.00	0.00	0.00	0.00
HCO ₃ ⁻ (mg/L) ¹	15.50	20.50	-	19.50	31.00	18.50	31.50	19.50	16.50	23.50	21.50	34.50
NH ₄ ⁺ (mg/L) ¹	<0.001	0.03	<0.001	<0.001	0.18	<0.001	0.00	<0.001	<0.001	<0.001	<0.001	1.09
NO ₂ ⁻ (mg/L) ¹	<0.001	<0.001	<0.001	<0.001	<0.001	<0.001	<0.001	<0.001	<0.001	<0.001	<0.001	<0.001
NO ₃ ⁻ (mg/L) ¹	0.06	0.01	0.02	0.03	0.11	0.08	0.21	<0.001	0.02	0.47	0.01	3.12
PO ₄ ³⁻ (mg/L) ¹	<0.001	<0.001	<0.001	<0.001	<0.001	<0.001	<0.001	<0.001	<0.001	<0.001	<0.001	<0.001
Si (mg/L)	8.57	6.76	7.93	5.93	10.56	7.25	11.21	7.00	5.05	10.15	12.76	17.80
SO ₄ ²⁻ (mg/L)	2.77	6.61	3.05	5.27	45.35	2.03	3.19	2.58	1.16	3.11	2.27	9.86
Cl (mg/L)	23.18	37.16	22.49	36.64	37.30	19.63	28.67	19.08	9.96	30.17	14.86	78.29
F (mg/L)	0.01	0.01	0.00	<0.001	<0.001	<0.001	0.01	0.01	<0.001	0.03	0.01	0.13
Br (mg/L)	0.09	0.05	0.07	0.07	0.12	0.08	0.11	0.04	0.04	0.09	0.05	0.26
Na (mg/L)	12.44	16.73	10.53	14.78	25.12	9.97	14.55	10.33	6.04	15.11	9.62	29.97
K (mg/L)	0.27	0.60	0.29	0.44	1.14	0.29	0.62	0.30	0.21	0.49	0.25	1.87
Mg (mg/L)	1.00	2.17	1.21	2.08	2.15	1.43	2.25	1.34	0.57	1.86	0.97	5.84
Ca (mg/L)	0.90	4.88	3.06	5.15	14.61	3.47	5.36	1.62	0.75	3.22	1.36	9.25
Fe (µg/L)	39.54	36.20	52.90	52.50	51.62	39.23	40.82	39.39	40.22	65.96	183.60	100.88
Se (µg/L)	41.56	44.73	90.97	59.28	57.13	52.28	51.60	48.16	40.75	46.03	35.28	57.20
Cu (µg/L)	14.76	14.31	20.79	13.98	13.27	13.72	13.52	16.37	14.86	15.34	42.74	13.96
Al (µg/L)	2.94	8.92	3.61	11.49	2.48	1.24	3.57	4.18	6.98	21.26	87.79	20.72
Ti (µg/L)	2.28	11.50	18.27	12.88	38.23	7.68	12.54	3.99	1.99	7.87	4.27	22.14
Zn (µg/L)	5.02	1.71	3.53	3.24	6.06	1.02	0.99	1.52	4.02	14.41	9.70	1.37
V (µg/L)	0.77	0.64	4.31	0.37	1.54	0.53	0.86	0.82	0.77	2.14	2.08	2.66
P (µg/L)	1.53	<1	4.27	<1	2.21	<1	<1	<1	1.38	6.34	9.08	76.15
Cr (µg/L)	0.86	0.92	10.06	1.33	1.08	0.51	0.86	0.71	0.61	0.91	0.66	1.52
Mn (µg/L)	<1	<1	<1	<1	<1	<1	<1	1.33	<1	3.69	9.88	22.62
Ni (µg/L)	<1	<1	1.02	<1	1.85	<1	<1	<1	<1	<1	<1	1.29
As (µg/L)	<1	<1	<1	<1	1.28	<1	<1	<1	<1	<1	<1	<1
Pb (µg/L)	<1	<1	<1	<1	<1	<1	<1	<1	<1	<1	3.96	<1
Sb (µg/L)	<1	1.54	<1	<1	<1	<1	<1	<1	<1	<1	<1	<1
Co (µg/L)	<1	<1	<1	<1	<1	<1	<1	<1	<1	<1	<1	<1
Mo (µg/L)	<1	<1	<1	<1	<1	<1	<1	<1	<1	<1	<1	<1
Ag (µg/L)	<1	<1	<1	<1	<1	<1	<1	<1	<1	<1	<1	<1
Cd (µg/L)	<1	<1	<1	<1	<1	<1	<1	<1	<1	<1	<1	<1
Sn (µg/L)	<1	<1	<1	<1	<1	<1	<1	<1	<1	<1	<1	<1
Ba (µg/L)	<1	<1	<1	<1	<1	<1	<1	<1	<1	<1	<1	<1
Tl (µg/L)	<1	<1	<1	<1	<1	<1	<1	<1	<1	<1	<1	<1
B (µg/L)	<1	<1	<1	<1	<1	<1	<1	<1	<1	<1	<1	<1

Kit-Soil-SE, Kit-R1-S1, Kit-R-N3, OP2-Sed, AR-R1, AR-R2) was determined with the Bruker D8 Advance X-Ray Diffraction (XRD) instrument, using a Cu K α radiation source, at ITU-JAL X-Ray Laboratory. Analyses were performed within a 4-72° 2 θ angle interval, with a step size of 0.019° and a speed of 0.2 s/step. Evaluations were made using the Bruker DIFFRAC.SUITE Software EVA Module. Petrographical identifications of eight representative volcanic rock thin sections from three different localities were done to understand the compositional and textural/structural properties of Fildes and Ardley Volcanites that dominate most of King George Island.

The representative samples of lava and pyroclastic rock were collected from Kitiesh Lake to the north, Ardley Island to the east and Flat Top Peninsula to the west of the Fildes Peninsula of King George Island. The rock samples were categorised into major groups and thin sections of the selected rock samples of volcanic origin were prepared

for microscopic analysis. The rock samples were crushed with a hydraulic press and a jaw crusher and finally pulverized with a Retsch disc vibrating mill for mineralogical and geochemical analyses.

The element concentrations of the lake sediment, soil and rock samples were analyzed at ACME Laboratories by coupled ICP-MS/ES and XRF methods using the lithium borate melt (ACME LF 2000 package) and presented as major oxides and trace elements. The samples were dried and pulverized using an agate mortar.

2.6. Polycyclic Aromatic Hydrocarbons (PAHs) measurements

The concentrations of polycyclic aromatic hydrocarbons (PAHs) in the sediment and soil samples from Lake Kitiesh and OP2 were packed in aluminum foil and stored in an ultra-freezer at -80 °C until analysis. EPA method 3550C was used for the extraction process (EPA, 2007).

Approximately 2–5 g of the wet sediment was weighed and mixed with anhydrous sodium sulfate (previously heated at 500 °C for 5 h) until the mixture became a free-flowing powder. The mixture was then transferred to a glass vial and 9–10 dimethylanthracene was sprinkled into the mixture as a surrogate standard. The extraction was carried out in triplicate using an acetone/hexane mixture. The extract (96 mL) was concentrated to a volume of about 1–2 mL.

EPA method 3630C was used for the cleaning process (EPA, 1996). In the purification step, a silica gel column was plugged with a small amount of glass wool, filled and emptied with DCM (dichloromethane) before use. The column was then filled with 10 g of silica gel (previously heated at 130 °C for 16 h) and topped up with approximately 1 cm of anhydrous sodium sulphate. Subsequently, 40 mL of hexane was poured in and drained at a rate of 2 mL min⁻¹. The extracted sample was transferred to the column and then the column was eluted with 25 mL of hexane and discarded. The aromatic fraction was removed by eluting the column with a 25 mL hexane: DCM (3:2) mixture was eluted. Then the concentrated extract was transferred to a 1 mL HPLC vial and 100 µL dimethylformamide was added as a keeper solvent. The extract was evaporated to dryness under a gentle stream of purified nitrogen gas and then made up to 1 mL with acetonitrile.

Fifteen PAHs were selected as priority pollutants (see Table 4). The PAH compounds were separated using a ZORBAX Eclipse PAH column (3.0 × 250 mm, 5 µm) with a guard column (4.6 × 12.5 mm, 5 µm) and analyzed by high performance liquid chromatography (HPLC) with a fluorescence detector (FLD). The column temperature was 25 °C and the injection volume was 10 µL. The flow rate of the mobile phase was 0.850 mL/min. A single excitation wavelength (260 nm) and multiple emission wavelengths (352, 420, 460, 495 nm) were used for the analyses. The elution gradient was programmed as water: acetonitrile 60:40 at 0–17 min; 0:100 at 17–25 min; 60:40 at 27–30 min.

The method was applied to spiked blanks (standards spiked in solvent) and a standard reference material from the National Institute of Standards and Technology (NIST) (SRM-1941b). The recoveries of the PAHs in SRM-1941b were between 67 % and 108 % of the certified values, with the exception of four of them (120 % for chrysene and benzo(b)fluoranthene; 173 % for dibenzo(a,h)anthracene; 131 % for benzo(ghi)perylene). The detection limits were between 0.01 and 0.05 µg/L, except for chrysene and benzo(ghi)perylene (0.5 µg/L), dibenzo(a,h)anthracene (2.5 µg/L) and indeno(123-cd)pyrene (1 µg/L).

2.7. Leaching experiments

Leaching experiments were conducted on the lake sediment, soil and rock samples to understand the mobilization of elements from the lake sediments and surrounding lithology into the water. Five samples, including two lake sediments (Kit-Sed, OP2-Sed), one soil (Kit-Soil-SE) and two rocks (Kit-R-S1, AR-R2) from Fildes and Ardley were used for the experiments. Prior to the experiments, the sediment, soil and rock samples were dried at 80 °C and ground to powder using an agate mortar. The leaching experiments were carried out with the ground samples in vitro in ultrapure water.

Experiments were performed in 50 mL sterile centrifuge tubes with a pulp density of 1:100 (g/L), by mixing 0.3 mg of the samples in 30 mL of water. Experiments were run for 1 h, 1 day, 1 week, and 2 weeks. The sample-solvent mixtures were rotated during the experiments using a Stuart STR4 Rotator Drive in the cold room (4 °C) of the ITU MOBGAM laboratories. The pH of the ultrapure water was measured prior to the experiments (approximately pH 5.48) and later the pH of the leachates was measured at the end of each experiment using a WTW InoLab pH meter. The samples were then centrifuged for 10 min at 6 °C and 4500 rpm at the end of the leaching experiments and the leachates were filtered using 0.2 µm syringe filters.

The concentrations of dissolved NH₄⁺, NO₂⁻, NO₃⁻, PO₄³⁻, SO₄²⁻, Cl⁻ and F⁻ in the leachate solutions were measured spectrophotometrically by using a Hach DR2800 spectrophotometer at the ITU

Geomicrobiology-Biogeochemistry Laboratory following the protocols provided by the test kits. Hach test kits based on the range of concentrations were; 0.01–2.0 mg/L for NH₄⁺ (Hach Code #2668000), 0.001–0.3 mg/L for NO₂⁻ (Hach Code #2107169), 0.01–10.0 mg/L for NO₃⁻ (Hach Code #2106169), 0.01–2.5 mg/L for PO₄³⁻ (Hach Code #2106069), 0.01–70.0 mg/L for SO₄²⁻ (Hach Code #2106769), 0.01–2.0 mg/L for Cl⁻ (Hach Code #2105569), 0.01–2.0 mg/L for F⁻ (Hach Code #2506025). Standard deviations in leaching experiments were calculated based on replicate measurements.

The alkalinity of the leachate was expressed as the sum of the concentrations of carbonate (CO₃²⁻) and bicarbonate (HCO₃⁻) determined by titration according to the standard method SM 2320 using 0.01 N sulphuric acid and methyl orange. The concentrations of Br⁻ were measured by IC and the concentrations of dissolved cations including Si, Na, Ca, K, Mg, Fe, Al, Mn, Sr, Ti, Ni, Cd, Zn, Cu, Ba, V, Mo, Co, As, B, Cr, Pb, Sb, Li and Be in the leachates were measured by ICP-MS as described in Section 2.4.

3. Results

3.1. Phytoplankton cell numbers

The total concentration of phytoplankton cells was 15 cells/mL in Lake Kitiessh (L2) and 206 cells/mL in the water sample OP2. The phytoplankton cell concentrations were in agreement with the chlorophyll-a values, with higher chlorophyll-a concentrations found in OP2 compared to Kitiessh Lake (Table 2). Analysis of phytoplankton species showed that the phytoplankton community was dominated by pennate diatoms, which were mainly 2–20 µm in size. In addition, a dinoflagellate species *Dissodinium* sp. was found in Lake Kitiessh.

3.2. Lake water ion composition

The ion concentrations measured in the water samples are shown in Table 2. The standard deviations of the ion concentrations in the lake water were calculated on the basis of two replicate measurements of the water sample from Kitiessh. Accordingly, the standard deviations for the IC measurements were NH₄⁺ ± 0.01 mg/L, SO₄²⁻ ± 0.03 mg/L, Cl⁻ ± 0.07 mg/L, F⁻ ± 0.01 mg/L, and Br⁻ ± 0.02 mg/L (NO₂⁻, NO₃⁻, PO₄³⁻ were below the detection limits). And the standard deviations of the ICP-MS measurements were: Na⁺ ± 0.28 mg/L, K⁺ ± 0.03 mg/L, Mg²⁺ ± 0.06 mg/L, Ca²⁺ ± 0.17 mg/L, Al³⁺ ± 0.63 µg/L, and below 1 µg/L for Si⁴⁺, P³⁺, Ti⁴⁺, V⁵⁺, Cr⁶⁺, Mn⁴⁺, Fe³⁺, Co²⁺, Ni²⁺, Cu²⁺, Zn²⁺, As³⁺, Se⁶⁺, Pb²⁺, Sb⁵⁺, Mo⁶⁺, Ag⁺, Cd²⁺, Sn²⁺, Ba²⁺, Tl³⁺, B³⁺.

The concentration of dissolved sulfate (SO₄²⁻) was highest in L4 (45.35 mg/L), while it ranged from 1.16 mg/L to 6.61 mg/L in the other lakes and ponds. The highest concentrations of chlorine (Cl⁻) were measured in OP2 (78.29 µg/L), while they ranged from 9.96 to 37.30 mg/L in the other samples. The concentrations of fluorine (F⁻) and bromine (Br⁻) ranged between <0.01–0.13 mg/L and 0.04–0.26 mg/L, respectively, and the highest concentrations were measured in OP2. Dissolved silica (Si) concentrations ranged from 5.05 to 17.80 mg/L, with the highest concentration measured in OP2. Higher concentrations of sodium (Na), potassium (K), magnesium (Mg), and calcium (Ca) were also found in L4 and OP2. Accordingly, the range of concentrations of Na was 6.04–29.97 mg/L, K was 0.21–1.87 mg/L, Mg was 0.57–5.84 mg/L, and Ca was 0.90–14.61 mg/L.

The concentrations of iron (Fe) were relatively higher in the organic ponds OP1 (183.6 µg/L) and OP2 (100.88 µg/L). Higher selenium (Se), copper (Cu), and chromium (Cr) concentrations were found in the Babylon stream water, 20.79 µg/L, 10.06 µg/L, and 90.97 µg/L. In the water samples, the values for aluminum (Al) ranged from 1.24 to 87.79 µg/L (highest in OP1), titanium (Ti) 1.99–22.14 µg/L (highest in L4), zinc (Zn) 0.99–6.6 µg/L (highest in L4) and vanadium (V) 0.53–2.66 µg/L (highest in OP2).

The concentrations of dissolved (P) were below the detection limit in

L2, L3, L5, L6 and P1 and varied considerably, with the highest concentration found in OP2 (76.15 µg/L), and ranging from 1.38 to 9.08 µg/L in the other samples. Some of the cations could be detected only in a few water samples. Manganese (Mn), for example, was detected in four water samples, with higher concentrations in OP2. The Mn concentration in P1 was 1.33 µg/L, P3 was 3.69 µg/L, OP1 was 9.88 µg/L and OP2 was 22.62 µg/L. The concentration of nickel (Ni) was also only measured in three samples: Babylon (1.02 µg/L), L4 (1.85 µg/L) and OP2 (1.29 µg/L). Arsenic (As) was only measured in L4 (1.28 µg/L), lead (Pb) was only detected in OP1 (3.96 µg/L) and antimony (Sb) only in L2 (1.54 µg/L). Cobalt (Co), molybdenum (Mo), silver (Ag), cadmium (Cd), tin (Sn), antimony (Sb), barium (Ba), thallium (Tl) and boron (B) were below the detection limit of 1 µg/L in all lakes and ponds (Table 2).

3.3. Mineral composition

Twenty different minerals were found in the XRD measurements (Table 3). Quartz and albite were the most common minerals found in most samples. Calcite and dolomite as well as the clay minerals montmorillonite, kaolinite, illite and smectite were most abundant in the samples from and near Lake Kitish. Alteration product minerals such as the zeolites, chabazite and faujasite were also found in the samples. Sample AR-R2 from Ardley Island had the greatest variety of minerals, enriched in quartz, clay minerals (e.g. montmorillonite), zeolites (e.g. chabazite, faujasite), metal oxides (e.g. magnanite) and hydrous metal oxides (e.g. birnesite) (Table 3).

3.4. Petrography of rock samples

The samples collected in the Kitish Lake littoral zone and near Flat Top Peninsula consisted mainly of basalt, basaltic andesitic and basaltic trachyandesitic lavas, whereas the samples from Ardley Island consisted mainly of pyroclastic rocks formed from volcanic breccias and agglomerates associated with andesitic-basaltic and andesitic lavas (Fig. 2). The basaltic lavas contained a modal composition of 80–85 % plagioclase (labradorite-bytownite), 7–10 % orthopyroxene, 3–5 % clinopyroxene, 1–5 % olivine and 1–2 % opaque mineral, while basaltic andesites and basaltic trachyandesites had 75–80 % plagioclase (andesine-labradorite), 5–10 % orthopyroxene and 5–7 % clinopyroxene, accompanied by sanidine phenocrysts (1–15 %) in basaltic trachyandesites.

Table 3

Mineralogical composition (XRD) of sediment, soil, and rock samples from Fildes Peninsula and Ardley Island. * Kit-Sed, Kit-Soil-SE, Kit-R-S1, OP2-Sed and Ar-R2 were used in the leaching experiments.

Mineral	Formula	Kit-Sed*	Kit-Soil-SE*	Kit-R-S1*	Kit-R-N3	OP2-Sed*	AR-R1	AR-R2*
Quartz	SiO ₂	+	+	+	+	+	+	+
Montmorillonite	(Na,Ca) _{0.3} (Al,Mg) ₂ Si ₄ O ₁₀ (OH) ₂ · n(H ₂ O)	+	+					+
Kaolinite	Al ₂ Si ₂ O ₅ (OH) ₄	+	+					
Illite	K _{0.65} Al _{2.0} (Al _{0.65} Si _{3.35} O ₁₀)(OH)							+
Smectite (Montmorillonite)	(Ca, Mg) _{0.33} Al ₂ Si _{3.67} A _{0.33} O ₁₀ OH ₂							+
Albite (Feldspar)	Na(AlSi ₃ O ₈)	+	+	+		+	+	+
Calcite	Ca(CO ₃)	+	+	+	+			+
Dolomite	Ca,Mg(CO ₃) ₂		+	+				
Augite (Pyroxene)	(Si, Al) ₂ O ₆			+				
Diopside (Pyroxene)	MgCaSi ₂ O ₆					+		+
Olivine	(Mg, Fe) ₂ SiO ₄			+				
Aluminum Calcium Sodium Silicate Hydrate	AlCaNaO ₄ Si ⁺² · H ₂ O				+			
Caoxenite (Aluminum Phosphate)	Fe ₃₊₂₄ Al(PO ₄) ₁₇ O ₆ (OH) ₁₂ · 17(H ₂ O)							
Chabazite (Zeolite)	(K ₂ ,Ca,Na ₂ ,Sr,Mg) ₂ [Al ₂ Si ₄ O ₁₂] ₂ · 12H ₂ O							+
Faujasite (Zeolite)	(Na ₂ ,Ca,Mg) 3.5 [Al ₇ Si ₁₇ O ₄₈]							+
Birnesite	(Mn ⁴⁺ ,Mn ³⁺) ₂ O ₄ · 1.5H ₂ O						+	
Manganite	(Bi,Ca)MnO ₃							+
Serpentine	(Mg,Fe,Ni, Mn,Zn) ₂₋₃ (Si,Al,Fe) ₂ O ₅ (OH) ₄							+
Sodalite	Na ₈ (Al ₆ Si ₆ O ₂₄)Cl ₂							+
Biotite	K(Mg,Fe) ₃ (Al,Fe)Si ₃ O ₁₀ (OH,F) ₂						+	

Rock samples from different locations showed similar compositions with different petrographic textural properties. Three different plagioclase generations were identified in the lavas of all compositions: 1) anhedral, corroded crystals with sieve textures, 2) euhedral-subhedral non-corroded clean crystals, and 3) microcrystals/microlites. Both clinopyroxene and orthopyroxene coexist with olivine as mafic phenocrysts within the basaltic lavas. All lava samples displayed hemi-crystalline porphyritic texture. The groundmass of these lavas was microlithic. Microlithic matrix was pilotaxitic, intersertal, or trachytic in character. Some of the samples, especially basalts, showed also vesicular and amygdaloidal textures; where the vesicle-filling minerals consisted of chalcedony/cristobalite, zeolite, and calcite (Supplementary Fig. S1a, b; Fig. S2c, d). A cumulo-phryic texture formed from plagioclase and pyroxene clusters was also observed in the lavas (Supplementary Fig. S1c, d). Some pyroxene crystals displayed twinning, and enclose plagioclase crystals forming poikilitic textures (Supplementary Fig. S1e, f).

The observations on thin sections showed that most of the rock samples from Kitish had gone through alteration, which affected both the minerals and the groundmass Fig. 2. In most of the samples, calcitization, sericitization, epidotization, and opacitization could be observed. Plagioclase phenocrysts were altered to calcite and sericite. Pyroxene crystals were mostly altered to chlorite, epidote, and calcite. Alteration products of olivine in basaltic rocks were chlorite, *serpentine* and *iddingsite*, and iron oxides. Some pyroxenes and olivine crystals were pseudomorphed by calcite or opaque mineral.

Volcanic breccias (flow breccias) and agglomerates found predominantly on Ardley Island consisted of basaltic, andesitic and andesitic lava fragments. The fragments in the volcanic breccias are angular/sub-angular in shape and up to 2 cm in size. Agglomerates were formed from rounded lava and pyroclastic fragments within the ash matrix. Flow breccias were formed from andesitic-basaltic andesitic lava fragments found in a hyalopilitic lava groundmass of similar composition (Supplementary Fig. S2 e, f). Opacitization was widespread in the mafic phenocrysts and matrix.

3.5. Element concentrations in the sediment, soil, and rock samples

The element compositions, mean detection limits and standard deviations for the ICP-MS analyses are listed in the supplementary Table S2. The SiO₂ contents in the sediment and soil ranged from 45.8 to

52.98 ± 0.1 %, with lower values in the Kitiesh samples. The Al₂O₃ content ranged from 16.19 to 19.80 ± 0.08 %, with the lowest values found in the Ardley Island OP2 sample. The weight percentages of Fe₂O₃ ranged from 7.92 to 9.69 ± 0.00 % (mean 7.80 %), MgO from 4.38 to 4.45 ± 0.03 % (mean 4.08 %), CaO from 3.06 to 6.94 ± 0.03 % (mean 5.31 %), Na₂O from 1.61 to 3.73 ± 0.03 % (mean 5.51 %), K₂O from 0.40 to 1.21 ± 0.01 % (mean 0.71 %), TiO₂ in the range of 0.70–1.63 ± 0.00 % (mean 0.9 %), P₂O₅ in the range of 0.09–1.00 ± 0.01 % (mean 0.24 %), MnO in the range of 0.13–0.016 ± 0.00 % (mean 0.13 %) and Cr₂O₃ in the range of 0.004–0.007 ± 0.0028 % (mean 0.05 %) in sediment and soil samples.

The sediment and soil samples from Kitiesh generally had lower contents of SiO₂ and Na₂O (Table 6). The highest K₂O content was found in the P2-Sed. OP2-Sed from Ardley Island had higher weight percentages of CaO, TiO₂ and P₂O₅. The differences in MnO content between the samples were negligible (standard deviation of 0.02 %). The total organic carbon (TOT/C) values in the sediments and soils ranged from 0.17 % to 1.51 %, with the highest levels found in the Kit-Sed and OP2-Sed. Total sulfur (TOT/S) was higher in Kit-Sed, L4-Sed and OP2-Sed (0.14 %, 0.12 % and 0.17 %, respectively) and ranged between 0.02 and 0.17 % for all samples (Supplementary Table S2).

The abundant trace elements in sediment and soil samples were: Sr (319–552 ± 1.6 ppm), V (188–263 ± 1.6 ppm), W (<0.5–252.3 ± 0.07 ppm), Ba (121–262 ± 4.24 ppm), Zr (63.2–163.4 ± 1.2 ppm) and Co (26.8–55.1 ± 0.4 ppm). The concentrations of Sc, Ni, Ce, Ga, Y, and Nd ranged between 7.4 ppm and 27.0 ppm (standard deviations ranging ±0.00–4.24 ppm; Table S2), while lower concentrations of La, Rb, Dy, Sm, Pr, and Hf ranged between 1.4 ppm and 13.4 ppm (Table S2). Concentrations of Yb, Er, Th, Eu, Cs, Tm, Lu, and Ta were below 2 ppm. Be and Sn detected only in Kit-Sed (Be and Sn 2 ± 0.2 ppm), L6-Sed (Be 2 ± 0.2 ppm), and OP2-Sed samples (Sn 2 ± 0.2 ppm).

In the rock samples, the contents of SiO₂ ranged 48.59–50.82 ± 0.1 %, Al₂O₃ ranged 18.82–21.29 ± 0.08 %, MgO ranged 2.76–4.30 ± 0.03 %, CaO ranged 7.54–12.14 ± 0.03 %, Na₂O 2.62–5.05 ± 0.03 %, K₂O ranged 0.18–0.97 ± 0.01 % (Table S2).

The geochemical findings were consistent with the petrographic results. Large Ion Lithophile (LILE) elements were enriched in all samples concerning High Field Strength Elements (HFSE) (Supplementary Fig. S3a). Also, Light Rare Earth Elements (LREE) were enriched in all samples compared to the Heavy Rare Earth Elements (HREE)

(Supplementary Fig. S3a). Lava geochemistry was determined by using the four selected samples with relatively low loss of ignition (LOI), which were Kit-R-S1, Kit-R-SE2, Kit-R-N4, and Kit-R-E1 (Table S2). By using the total alkali (Na₂O+K₂O) versus silica (SiO₂) content of the samples, the composition of the lava was plotted in the TAS-Diagram showing that the samples were basalt and trachy-basalt in composition (Fig. 3).

3.6. PAHs

The total PAHs in the samples ranged between 9.55 and 131.25 ng g⁻¹ dry weight (dw), where the generally highest values belonged to Bab-Sed and Kit-Soil-NW (Table 4). Due to the limited amount of sample material, standard deviations for PAH measurements were calculated based only on replicate samples of Kit-sed samples (*n* = 2); *Naphthalene* (12.32 ± 0.16 ng g⁻¹ dw), *Pyrene* (0.09 ± 0.07 ng g⁻¹ dw), *Chrysene* (1.25 ± 0.07 ng g⁻¹ dw), and *Benzo(ghi)perylene* (0.39 ± 0.23 ng g⁻¹ dw). The lowest total PAHs belonged to the sample collected inside the Kitiesh Lake, Kit-Sed (–10 m) (Table 4). *Phenanthrene* (*Phe*) was found as the dominant PAH, especially in the sediment sample of Babylon stream and Kit-Soil-NW and Kit-Soil-SE samples. *Naphthalene* (*Nap*) was found in all samples except for the Kit-Soil-NE sample. The concentrations of *Fluorene* (*Fl*) were higher in Bab-Sed, Kit-Soil-NW, and Kit-Soil-SE. The levels of *Benzo(a)pyrene* (*Bap*), *Fluorene* (*Fl*), and *Naphthalene* (*Nap*) were comparatively higher in the Bab-Sed sample.

3.7. Leachate pH, anion and cation concentrations

In Fig. 4, the changes in pH, anions and cations in the leaching experiments were plotted against the contact times of the sample with the water: t₀=0-h, t₁ 1-h, t₂ 24-h, t₃ 168-h (1-week) and t₄ 336-h (2-weeks). Also, the maximum leached amounts of elements (Si, Al, Fe, Mg, Ca, Na, K, Ti, P, Mn, Cr, S, Ba, Ni, Co, Sr) were compared with the element content in the samples in Table 6.

The pH values in the experiments generally increased in 1-h and fell below the initial level in 1-week (pH 4.2 and pH 4.9, respectively) and gradually increased in the 2-weeks experiments (Fig. 4). The highest pH values above 9 were found in the leaching tests with the rock samples (Fig. 4). The pH in Kit-R-S1 in the 1-h experiments were average 9.55 ± 0.07 and AR-R2 in the 1-h experiments were pH average 9.77 ± 0.02. pH

Table 4

Polycyclic Aromatic Hydrocarbons (PAHs) concentration of soil and sediment samples from Kitiesh Lake, Babylon stream, and OP2, determined by HPLC-FID analyses. nd; not detected.

PAH (ng g ⁻¹ dw)	Kit-Sed	Bab-Sed	Kit-Soil-NE	Kit-Soil-SE	Kit-Soil NW	Kit-Soil-SE	OP2 Sed	Total (ng g ⁻¹ dw)
<i>Naphthalene</i>	12.32 ± 0.16	3.45	0.00	4.35	9.44	7.47	3.60	40.63
<i>Acenaphthene</i>	0.00	4.79	0.00	0.00	1.79	7.02	0.00	13.60
<i>Fluorene</i>	0.00	11.78	0.90	3.89	16.51	10.97	2.18	46.23
<i>Phenanthrene</i>	0.00	92.84	0.00	0.00	100.54	58.46	3.40	255.24
<i>Anthracene</i>	0.00	0.00	0.00	0.00	0.00	0.00	0.00	0.00
<i>Fluoranthene</i>	0.00	0.00	0.00	0.00	0.00	0.00	0.00	0.00
<i>Pyrene</i>	0.09 ± 0.07	0.00	0.11	0.00	nd	0.00	0.04	0.24
<i>Benzo(a)anthracene</i>	0.00	nd	nd	nd	nd	nd	nd	0.00
<i>Chrysene</i>	1.25 ± 0.07	1.99	0.95	0.78	nd	nd	nd	4.79
<i>Benzo(b)fluoranthene</i>	0.00	0.00	0.00	0.00	0.00	0.00	0.00	0.00
<i>Benzo(k)fluoranthene</i>	0.00	0.00	0.00	0.00	0.00	0.00	0.00	0.00
<i>Benzo(a)pyrene</i>	0.00	16.01	7.60	1.42	0.00	0.00	3.87	28.9
<i>Dibenzo(a,h)anthracene</i>	nd	nd	nd	nd	nd	nd	nd	0.00
<i>Benzo(ghi)perylene</i>	0.39 ± 0.23	0.39	nd	nd	nd	nd	0.01	0.79
<i>Indeno(123-cd)pyrene</i>	nd	nd	nd	nd	nd	nd	nd	nd
Total PAHs	14.04	131.25	9.55	10.44	128.28	83.93	13.09	390.58

values in the Kit-Sed in the 2-week experiments were average 7.75 ± 0.78, Kit-Soil in the 2-week experiments were 8.4 ± 0.42 (Fig. 4). The concentrations of CO₃²⁻, Li, Be, Se, and Sn in the leachates were below the

measurement limits. Total alkalinities were inferred from the bicarbonate (HCO₃⁻), which increased up to 90.25 ± 0.94 mg/L from the initial level of ultrapure water of 6.5 mg/L. The HCO₃⁻ values were higher in the experiments with the all the rock samples and at lower levels

in the sediment and soil samples from Kitiash Lake (Fig. 4).

The highest rates of fixed nitrogen were released in the form of NH_4^+ from Kit-Soil-SE and OP2-Sed (1.81 ± 0.00 mg/L, 0.62 ± 0.04 mg/L, respectively). The NH_4^+ values were reduced below the initial values of DI water in the 2-week experiments. NO_3^- was also released into the water in all experiments, with the highest input from the Kit-Sed and Kit-Soil-SE (0.97 ± 0.01 mg/L, 0.54 ± 0.01 mg/L, respectively). NO_3^- concentrations were increased in all samples, then gradually decreased except for the OP2 (0.4 ± 0.01 mg/L). On the other hand, NO_3^- release from the rock samples Kit-R-S1 and AR-R-2 remained stable after the initial increase (Fig. 4). The values of the other nitrogen component nitrite (NO_2^-) were below the detection limit, except for Kit-Sed and Kit-Soil-SE (0.32 ± 0.03 mg/L, and 0.92 ± 0.04 mg/L, respectively).

Phosphate (PO_4^{3-}) was released in all samples. The highest phosphate was released from OP2 (1.03 ± 0.04 mg/L). Phosphate input from the samples generally increased in the 1-h and 24-h experiments and decreased thereafter. The lowest PO_4^{3-} release was observed in the Kit-Soil. Sulphate (SO_4^{2-}) was the anion that was released the most in the leaching experiments, reaching a value of 23.50 ± 2.12 mg/L in OP2 in the 24-h experiment. The highest barium (Ba) values were found in the Kit-Sed 1-h experiments at 20.39 ± 0.51 $\mu\text{g/L}$ and in the OP2-Sed at 11.68 ± 3.6 $\mu\text{g/L}$.

The highest zinc (Zn) levels observed in the experiments were 54.92 ± 7.53 $\mu\text{g/L}$ in Kit-Sed. The increase in copper (Cu) concentrations showed a relatively more regular profile compared to Zn (Fig. 4). The highest Cu value in the experiments was 25.36 ± 4.25 $\mu\text{g/L}$ (Kit-R-S1), cobalt (Co) 12.35 ± 0.56 $\mu\text{g/L}$ (AR-R2), vanadium (V) 14.49 ± 68 $\mu\text{g/L}$ (OP2-Sed). Kit-Sed sample showed a high release of arsenic (As) (9.16 ± 5.91 $\mu\text{g/L}$). Lead (Pb) was released in all leaching experiments. Pb release ranged from 1.12 to 2.17 ± 0.39 $\mu\text{g/L}$ with the highest values in the Kitiash samples (Fig. 4). Chromium (Cr) and antimony (Sb) were only leached from the Ardley Island samples.

4. Discussion

4.1. Lake pH and alkalinity

Changes in pH can affect phytoplankton community structure in Antarctic marine lakes on the Fildes Peninsula and Ardley Island. The results of the leaching experiments with sediment, soil and rock samples showed a general trend of increasing pH by up to 4 pH units to pH values up to 9.7, except for the one-week experiments with Kit-Sed and Kit-Soil (Fig. 4). The increase in pH in the lakes was also evidenced by the observations. For example, the average pH of five lakes on the Fildes Peninsula (of L2, L3 and L5 as common lakes) averaged 6.0 ± 0.1 based on measurements in 1998 (Perendez and Carrasco, 2003). While the measured pH values in 2017 in this study averaged 8.2 ± 0.6 (Table 2). An increase in ice melt and liquid precipitation in the region could cause the leaching of basic rocks of basalt and trachy-basalt, which affects the pH of the lakes. The alkalinity in the leaching experiments, which can be derived from the HCO_3^- concentrations, also increased (Fig. 4).

The changes in pH and alkalinity could also be due to the dissolution of carbonates in the form of calcite and dolomite minerals, which were abundant in the samples (Table 3) and reflected in an increase in Ca and Mg in the leachates (Fig. 4). With global warming and increasing liquid precipitation in the summer season, lakes in the region may become more alkaline. For example, the region experienced relatively high precipitation in January, February and March 2017 (> 3 mm), with the largest precipitation event occurring in January (<https://rp5.ru/>). The potential increase in pH may be mitigated to some extent by the increase in atmospheric CO_2 concentration, which is known to acidify the aquatic environment through the formation of carbonic acid (H_2CO_3) (Caldeira and Wickett, 2003).

4.2. Macronutrients N, P, and Si

The Pearson correlation between the dissolved elements and other characteristics of the lakes is shown in Table 5. High positive correlations were found between the chl-a concentrations and NO_3^- , NH_4^+ , F, P, and Mn (Table 5). Based on the chl-a levels, the studied lakes ranged from ultra-oligotrophic to mesotrophic as lakes L1–6 and ponds P1–3 had low chl-a concentrations (<1.5 $\mu\text{g/L}$), while organic ponds OP1 and OP2 had chl-a concentrations >2.5 $\mu\text{g/L}$ (Table 2). In addition, the number of phytoplankton cells in OP2 (206.4 cells/L) was significantly higher than in L2 (14.8 cells/L). OP2 was also the lake with the highest chlorophyll-a levels (Table 2). The fixed nitrogen species NO_3^- , NO_2^- , NH_4^+ and PO_4^{3-} together with Si are the most important macronutrients necessary for phytoplankton growth. Primary production in lakes is generally considered to be P-limited, while N-limitation is more common in ocean waters (Wetzel, 2001). Dissolved NO_3^- in the lake water samples ranged from 0.001 to 3.12 mg/L, dissolved NO_2^- was below detection, dissolved NH_4^+ ranged <0.001 –0.18 mg/L, and dissolved Si ranged from 5.05 to 17.80 mg/L (Table 2). PO_4^{3-} concentrations were below the detection limit of 0.001 mg/L in all samples, indicating a possible P-limitation in the lakes studied. A significant release of PO_4^{3-} was observed in the leaching experiments (Fig. 4). The highest PO_4^{3-} release of 1 mg/L was observed in the sediment sample OP2 on the Ardley Island.

Chemical weathering is responsible for the N and P input into the study region and thus into the lakes. Fertilization of Antarctic lakes has been previously demonstrated by an increasing trend in chlorophyll-a levels on Antarctic Signy Island (Qayle et al., 2002). NH_4^+ and NO_3^- are the most important nutrients for phytoplankton and their presence in the lakes influences primary production. Although PO_4^{3-} , the biologically utilizable form of P as a nutrient, is below detection limits, elemental P levels show a high correlation with chlorophyll-a levels (Table 5). Weak correlations were observed between the chlorophyll-a values and the area of the lakes, their distance from the shore, the distance from the glacier and the altitudes of the lakes (Table 5).

For this reason, the Si input into lakes can influence the species composition. The main source of dissolved Si in the leaching experiments could be the dissolution of Si-containing minerals such as montmorillonite, kaolinite, albite and pyroxene (Table 3). The predominant phytoplankton species in the studied lakes were diatoms with common species such as *Achnanthes dolomiticum*, *Nitzschia hamburugiensis*, *Planothidium lanceolatum*, *Craticula pseudocitrus*, *Fragilaria capucina* (Cura, 2020). The Si concentrations in the lakes showed a high

Table 6Element contents in the samples and the amounts leached to the water. Also shown is the R²: coefficient of determination content versus leached amounts.

			Kit-Sed	Kit-Soil-SE	Kit-R-S1	OP2-Sed	AR-R2	R ²
Si	Element content	SiO ₂ (%)	45.80	47.24	48.64	51.90	68.93	
	Leached amount	Si (mg/L)	63.01	53.09	76.32	3.16	3.02	-0.73
Al	Element content	Al ₂ O ₃ (%)	17.75	19.80	19.06	16.19	13.00	
	Leached amount	Al (μg/L)	908.63	822.59	484.31	364.84	639.06	0.25
Fe	Element content	Fe ₂ O ₃ (%)	9.28	9.27	8.72	8.38	4.59	
	Leached amount	Fe (mg/L)	1.16	0.93	1.42	0.30	0.55	0.48
Mg	Element content	MgO (%)	4.38	4.45	3.66	3.51	1.73	
	Leached amount	Mg (mg/L)	1.06	0.99	2.75	2.25	0.84	0.13
Ca	Element content	CaO (%)	5.01	4.71	12.14	6.45	1.40	
	Leached amount	Ca (mg/L)	2.34	1.52	5.82	5.15	14.31	-0.38
Na	Element content	Na ₂ O (%)	1.61	1.78	2.62	3.73	3.50	
	Leached amount	Na (mg/L)	2.21	0.68	3.24	20.89	19.50	0.94
K	Element content	K ₂ O (%)	0.44	0.44	0.26	0.75	0.74	
	Leached amount	K (mg/L)	0.90	1.57	2.01	0.52	1.05	-0.81
Ti	Element content	TiO ₂ (%)	0.72	0.70	0.76	1.63	0.61	
	Leached amount	Ti (μg/L)	27.69	15.22	23.04	35.22	49.24	-0.60
P	Element content	P ₂ O ₅ (%)	0.23	0.09	0.11	1.00	0.14	
	Leach	P ₂ O ₄ (mg/L)	0.04	0.01	0.07	0.67	0.07	0.12
Mn	Element content	MnO (%)	0.14	0.13	0.15	0.12	0.09	
	Leached amount	Mn (μg/L)	203.68	24.88	23.73	84.01	26.99	-0.17
Cr	Element content	Cr ₂ O ₃ (%)	0.01	0.01	0.01	0.01	0.01	
	Leached amount	Cr (μg/L)	0.60	0.64	0.00	3.59	3.44	-0.53
S	Element content	TOT/S (%)	0.14	0.04	<0.02	0.17	0.06	
	Leached amount	SO ₄ (mg/L)	11.50	1.40	0.00	20.25	1.00	0.97
Ba	Element content	Ba (ppm)	121.00	144.00	115.00	146.00	215.00	
	Leached amount	Ba (μg/L)	8.16	2.86	1.76	4.84	9.05	0.59
Ni	Element content	Ni (ppm)	26.00	<20	39.00	<20	<20	
	Leached amount	Ni (μg/L)	8.09	28.79	18.74	0.82	0.25	1.00
Co	Element content	Co (ppm)	30.10	26.80	41.40	55.10	22.00	
	Leached amount	Co (μg/L)	2.37	3.36	3.13	10.35	11.01	0.19
Sr	Element content	Sr (ppm)	344.10	319.00	511.80	396.80	324.20	
	Leached amount	Sr (μg/L)	28.52	48.87	12.81	57.96	32.03	0.92

lithologic samples during the leaching experiments. (Fig. 4) Fe release from the Kit-Sed and Kit-soil samples increased until the 1-week experiment and remained stable thereafter. Fe-release in the experiments showed a very similar pattern with Si. Other micronutrients such as Zn, Cu and Co were also released during the leaching experiments (Fig. 4). A higher release of Zn was observed in the lake sediments compared to soil and rock. The lake sediment samples Kit-Sed and OP2 released higher amounts of Mn and SO₄. The highest barium (Ba) concentrations ranged 2.23 μg/L to 20.39 μg/L and the highest values were observed in the lake sediments Kit-Sed and OP2-Sed.

Although Zn and Cu are nutritional elements, at high concentrations they can also have negative effects on phytoplankton. Similarly, a toxic suppressive effect has been observed for F. In culture experiments, F was found to suppress the toxic effect of Al (Ali, 2004). Mn is thought to reduce the cellular uptake of elements such as Zn, Cu, and Cd (Sunda and Huntsman, 1983; Sunda and Huntsman, 1995). Dissolved Mn in lakes showed a correlation with chlorophyll-a concentrations in P1, P3, OP1, and OP2 (Table 2). In the leaching experiments, Mn release from the lake sediments was higher than from the soil and rock samples. Mn-containing birnesite and manganite minerals may be the source of Mn in the leaching experiments (Table 6). In addition to minerals, bacterial activity may also play a role in the Mn cycle. Black radial encrustations observed in the rock sample AR-R2 indicate the presence of bacterial activity (Fig. 2). However, no correlation was found between the elemental contents of S and Mn in the samples and the their release rates in the leaching experiments (Table 6). The high amounts of SO₄²⁻ and Mn released into the water during the leaching experiments suggested that S and Mn cycling and diagenetic processes also play an important role in the study area.

Bacterial activity in lakes, soil and sediment can also affect dissolved nutrients. Total C values in the sediment and soil samples ranged from 0.17 % to 1.51 %, while total S values ranged from <0.02 % to 0.17 % (Table S2). The higher carbon values were measured in the lake sediments of Kitiash and OP2, while the higher sulfur values were measured

in the sediment samples of Kitiash, L4 and OP2. The correlation between total C values in the sediment samples and chl-a was lower than expected (R² = 0.67) (Table 5), which may be related to the loss of some of organic matter due to bacterial activity and its mineralization during the decomposition processes.

Marine aerosols (or sea salts, sea spray) are micrometer-sized salt particles that are formed by the action of waves. Therefore, the soil structure in the maritime Antarctic is characterized as salty soil (Hall et al., 1993). Especially in the summer season, when the ice and snow cover on the lakes disappears, a higher input of nutrients from the atmosphere is to be expected. High Ca, Sr, Ba and SO₄ values measured in the water sample from OP2 indicate a higher sea salt content in the soil (Table 2). The high Ca content in the lake water is likely due to coupled effects of rock weathering and sea spray deposition. Storms in the region can also affect dissolved solids, conductivity, and pH values in the lakes (Contreras et al., 1991). L2, L4 and OP2 had high conductivity values of over 200 μS cm⁻¹ (Table 2). The influence of the sea is higher in these lakes than in the others (Broady, 1989). Among these lakes, L4 (Langer Lake) has a connection to seawater through a small estuary which was also confirmed by the high sulfate values (45 mg/L) compared to the other lakes, which ranged from 1.16 mg/L to 9.86 mg/L (Table 2). L4 and the east coast of the Fildes Peninsula and parts of Ardley Island are more polluted by marine salt spray.

Lakes can be affected by pollution from the sea due to the deposition of sea spray. The input of seawater was reflected in the SO₄ and Ca values, while the input of sea spray was reflected in the Na, Cl and F values (Table 2). Leaching experiments showed the release of Na, Ca, Sr, Ba, Co, Cr, Sb, and Cd in the Ardley Island samples suggesting a marine influence (Fig. 4). On the other hand, the Kitiash Lake samples released high levels of Si, K, Al and Fe, which are terrestrial indicators (Fig. 4).

In the studied lakes, Chl-a levels decreased with increasing distance from the shore and increasing altitude. At the same time, the deposition of sea spray is expected to be higher in lakes with low elevation that are close to sea level. L1 (Uruguay) is the lake closest to the Collins Glacier

and has the lowest chl-a values (Fig. 1, Table 2). Lakes near glaciers tend to be younger in terms of outburst and may be exposed to white turbidity sediment pollution, referred to as 'glacial flour or glacial milk', which has detrimental effects on phytoplankton and zooplankton (Sommaruga, 2015). Therefore, primary production is generally considered to be lower in the early stages of para-glacial lakes (Sommaruga, 2015). The low production observed in L1 (Uruguay) may therefore support para-glacial processes.

4.4. Toxicity

Heavy metals, including those that are essential micronutrients (e.g. Zn, Cu, etc.), are toxic to phytoplankton in high concentrations (Rai et al., 1981). Heavy metals such as As, Ag, Cd, Pb, Ni, Al, Cr and Sn also have toxic effects on phytoplankton if they are present in excessive quantities (Hutchinson, 1973). The negative effects of Ni on freshwater phytoplankton have already been reported (Spencer and Greene, 1981). Ni-content in the samples ranged from <20 ppm to 39 ppm and the highest values were found in the rock samples Kit-Sed, Bab-Sed, L4-Sed, L6-Sed, and Kit-R-S1 (Table S1). Due to the high Ni content in the samples, the source of Ni in the lakes is more likely related to lithology. In the lakes analyzed, the dissolved concentrations of As, Mo, Ag, Cd, Sn, Sb, Ba, Tl, B, and Pb (with the exception of OP1) were mostly either low or below the detection limit (Table 2).

An enrichment of Zn and Cd in the lake waters of the Fildes Peninsula has previously been linked to the local anthropogenic pollution (Perendez and Carrasco, 2003). In our leaching experiments, no Cd was released from the Fildes Peninsula samples, whereas a higher input of Cd was detected from the Ardley Island samples (highest 0.8 µg/L; Fig. 4). However, leaching experiments indicated a possible influence of lithology on Cd enrichment. The Co, Cr and Sb dissolution in the leaching experiments was also significantly higher in samples from Ardley Island (Fig. 4). Therefore, the levels of Cd, Cr and Sb in the lakes were probably of lithologic origin rather than anthropogenic pollution. The heavy metals found in low concentrations in the leaching experiments were V, Mo, As, B, Cr, Pb, and Cd. Cr and Sb, on the other hand, were only leached from the samples from the Ardley Island (Fig. 4). The highest Cr values in the leachates were between 1.18 and 4.96 µg/L, Sb between 2.67 and 3.374 µg/L and Cd between 0.45 and 0.75 µg/L.

The most pronounced effects of pollution were observed in the dissolved Pb levels of OP1 (Table 2). The Pb concentration in the OP1 water sample was 3.96 µg/L, while it was below the detection limit in all other lakes analyzed. OP1 is located near onshore oil tanks and may have been affected by petroleum contamination (Fig. 1). The release Pb was also detected in the leaching experiments (Fig. 4). Pb was released from all samples in all leaching experiments. Pb release ranged from 1.12 µg/L to 2.17 µg/L with the highest values in the Kitesh samples (Fig. 4). Therefore, the main source of Pb enrichment in OP1 could be either pollution from oil tanks or natural input from lithology.

Hg, Se and Sb are also elements that are bioaccumulated by aquatic organisms. Hg was below the detection limit in both lake water and lake sediments, while Se (35.28–90.97 µg/L) and Sb (1.54 µg/L in L2 only) were found in the lake water samples (Table 2). The leaching experiments showed that the source of Se and Sb was not the lithology, as these two elements were not released into the water. Therefore, the possible source of Se and Sb can be either anthropogenic or ornithogenic.

Cl can also have negative effects on microorganisms as it disrupts the cell wall structure and damages the cell's DNA, which makes chlorination a common disinfection method. In the leaching experiments with Kitesh sediment and soil samples, the Cl content increased up to 2 mg/L in the 1-week leaching experiments (Fig. 4). The Cl increase in the experiments could also have affected the pH of the leachate and the bicarbonate content through the formation of hypochlorous acid (HOCl) and OCl⁻ and H⁺ ions. Cl may also have reacted with nitrogen compounds as the increase in NO₂⁻ and NO₃⁻ generally coincided with the increased Cl concentrations in the experiments (Fig. 4).

In the leaching experiments with Kitesh sediment and soil samples, the Cl content increased up to 2 mg/L in the 1-week leaching experiments (Fig. 4). The Cl increase in the experiments could also have affected the pH of the leachate and the bicarbonate content through the formation of hypochlorous acid (HOCl) and OCl⁻ and H⁺ ions. Cl might have also reacted with nitrogen compounds as the increase in NO₂⁻ and NO₃⁻ generally coincided with the increased Cl concentrations in the experiments (Fig. 4).

PAHs are harmful to freshwater phytoplankton and are known to have negative effects on growth, photosynthesis and the cell membrane (Ben Othman et al., 2023). PAHs accumulate in all environments, including soils and lakes, and can be of both natural and anthropogenic origin. *Benzo(a)pyrene* (Bap) is more toxic to phytoplankton, while the most water-soluble *naphthalene*, *acenaphthene* and *fluorene* are the least toxic PAHs (Ben Othman et al., 2023). Total PAHs in sediment and soil samples from the littoral zone and interior of Lake Kitesh and OP2 on Ardley Island ranged from 9.55 to 131.25 ng g⁻¹ dry weight (dw), with *Phenanthrene* being the dominant PAH (Table 4). A previous study of total PAH concentrations of soil samples collected from the Fildes Peninsula in 2016 found lower concentrations ranging from 1.83 to 32.9 ng g⁻¹ dw, with *Phenanthrene* and *Anthracene* being the most prominent PAHs in the soil samples (Deelaman et al., 2020). PAH concentrations were found to be higher in the samples around Great Wall Station and the road network indicating an anthropogenic source of PAHs in the region (Deelaman et al., 2020).

PAHs can also be delivered through long-range atmospheric transport and deposited in the remote Antarctic via wet and dry deposition. All types of PAHs, except *Benzo(a)pyrene*, were found in the snow samples collected in the Fildes Peninsula (Na et al., 2011). Although the PAH levels in the lake sediment samples were below the threshold toxic levels to phytoplankton of 10–1000 µg/L found in the literature (Ben Othman et al., 2023), their increasing accumulation with anthropogenic inputs in the Antarctic lakes may harm the phytoplankton.

Penguin droppings were also analyzed for heavy metal concentrations, as heavy metals bioaccumulate and are passed on by penguins. An earlier sediment core study on Ardley Island showed an increase in the input of anthropogenic Pb through bioaccumulation in the ocean and subsequent deposition in lake sediments with penguin feces (Sun and Xie, 2001).

5. Conclusions and recommendations

The results of this study show that the lithology on the Fildes Peninsula and Ardley Island in the Maritime Antarctic has a significant impact on lake biogeochemistry. Leaching experiments showed that pH can increase with increasing chemical weathering. The input of Si, N, P, Fe, Zn and Co from the lake sediments, soils and rocks may have the potential to fertilize the lakes and increase phytoplankton production in the lakes of maritime Antarctica. On the other hand, releases of Pb, Cu, Cd, Al and As may have toxic effects on phytoplankton, which could be partially reduced by the Mn content in the lakes and the high Mn mobilization from the surrounding lithology. Our study suggests that the P, S and Mn cycles play an important role in the biogeochemistry of Antarctic lake water. With melting, more rock surfaces are exposed and more proglacial lakes are formed, which may indicate an increasing role of lake ecosystems in the C cycle, as both chemical weathering and photosynthesis are important for the fixation of atmospheric CO₂. In addition, the duration of ice cover in the winter season will decrease as temperatures rise. This in turn may lead to an increased leaching of elements from the lithology and an increased input of nutrients such as N, P, Si and Fe into the Antarctic lakes.

CRedit authorship contribution statement

Nazlı Olgun: Conceptualization, Methodology, Investigation, Writing – original draft. **Ufuk Tar:** Methodology, Visualization, Writing

- review & editing. **Nurgül Balcı:** Conceptualization, Methodology, Writing - review & editing. **S. afak Altunkaynak:** Investigation, Writing - original draft. **Isıl Gürarlan:** Investigation, Writing - original draft. **Sevil Deniz Yakan:** Methodology, Writing - review & editing. **Frederic Thalasso:** Conceptualization, Methodology, Investigation, Writing - review & editing. **María Soledad Astorga-España:** Investigation, Writing - review & editing. **Léa Cabrol:** Methodology, Investigation, Writing - review & editing. **Céline Lavergne:** Investigation, Writing - review & editing. **Linn Hoffmann:** Investigation, Writing - review & editing.

Declaration of competing interest

The authors declare the following financial interests/personal relationships which may be considered as potential competing interests: N. Olgun reports financial support was provided by Technological Research Council of Türkiye. N. Olgun reports a relationship with Technological Research Council of Türkiye that includes: funding grants.

Data availability

Data will be made available on request.

Acknowledgments

This study was funded by the The Scientific and Technological Research Council of Türkiye (TÜBİTAK) Project #118Y372. Field expenses of N. Olgun were supported by Istanbul Technical University (ITU-BAP-Link2-Project #40265). F. Thalasso, M. S. Astorga-España, L. Cabrol, and C. Lavergne were supported by the Instituto Antártico Chileno (INACH) Project RT-14-15. C. Lavergne was also funded by the Chilean grant ANID FONDECYT #3180374 and the INACH project FP_07-18. We thank M. A. Kurt for ICP-MS measurements, Ezgi Tok and Cansu Demirel for assistance in leaching experiments, Yağmur Güneş for her assistance in XRD measurements, and Nadjeđa Espinel-Velasco for assistance in phytoplankton cell count. We further thank Prof. Dr. Jose Retamales, the INACH team in the Chilean Station Julio Escudero and Prof. Dr. Burcu Özsoy, and the ITU-POLREC team for their logistic support. This study was carried out under the auspices of the Presidency of The Republic of Türkiye, supported by the Ministry of Industry and Technology, and coordinated by TÜBİTAK MAM Polar Research Institute.

Appendix A. Supplementary data

Supplementary data to this article can be found online at <https://doi.org/10.1016/j.scitotenv.2023.168562>.

References

Alfonso, J.A., Vasquez, Y., Ahernandez, A.C., Mora, A., Handt, H., Sira, E., 2015. Geochemistry of recent lacustrine sediments from Fildes Peninsula. *King George Island, maritime Antarctica: Antarctic Science* 27 (5), 462–471.

Ali, G., 2004. Fluoride and aluminium tolerance in planktonic mikroalga: *Flouride* 37 (2), 88–95.

Bastviken, D., J. C., Pace, M., Tranvik, L., 2004. Methane emissions from lakes: dependence of lake characteristics, two regional assessments, and a global estimate. *Global Biogeochem. Cycles* 18, 1–12.

Ben Othman, H., Pick, F.R., Hlaïli, A.S., Leboulanger, C., 2023. Effects of polycyclic aromatic hydrocarbons on marine and freshwater microalgae - a review. *J. Hazard. Mater.* v, 441.

Birkenmajer, K., Zastawniak, E., 1989. Late Cretaceous-early Tertiary floras of King George Island. *West Antarctica: their stratigraphic distribution and palaeoclimatic significance: Geological Society, London, Special Publications* 47, p. 277–240.

Borrel, G., Je'ze'quel, D., Biderre-Petit, C., Morel-Desrosiers, N., Morel, J.P., Peyret, P., Fonty, G., Lehours, A.C., 2011. Production and consumption of methane in freshwater lake ecosystems. *Res. Microbiol.* 162, 832–847.

Broady, P.A., 1989. Broadscale patterns in the distribution of aquatic and terrestrial vegetation at three ice-free regions on Ross Island, Antarctica. *Antarct. Sci.* 1, 109–118.

Caldeira, K., Wickett, M.E., 2003. Anthropogenic carbon and ocean pH. *Nature* 425, 365.

Contreras, M., Cabrera, S., Montecino, V., Pizarro, G., 1991. Dinámica abiótica del lago Kitiash. *Antártica: Serie Científica INACH* 41, 9–32.

Cura, H., 2020. Identification of Antarctic freshwater diatom species by using microscopic and molecular techniques. In: Master Thesis, 85. Istanbul Technical University.

Deelaman, W., Pongpiachan, S., Tipmanee, D., Suttinun, O., Choochuay, C., Iadtem, N., Charoenkalunyata, T., Promdee, K., 2020. Source apportionment of polycyclic aromatic hydrocarbons in the terrestrial soils of King George Island. *Antarct. J. South Am. Earth Sci.* 104, 102832.

El Bilali, L., Rasmussen, P.E., Hall, G.E.M., Fortin, D., 2002. Role of sediment composition in trace metal distribution in lake sediments. *Appl. Geochem.* 17 (9), 1171–1181.

Emslie, S.D., Polito, M.J., Brasso, R., Patterson, W.P., Sun, L., 2014. Ornithogenic soils and the paleoecology of pygoscelid penguins in Antarctica. *Quat. Int.* 352, 4–15.

EPA, 1996. Method 3630C. Silica Gel Cleanup, United States Environmental Protection Agency.

EPA, 2007. Method 3550C Ultrasonic Extraction. Agency, United States Environmental Protection.

Fensterseifer, H.C., Soliani, E., Hansen, M.A.F., Troian, F.L., 1988. Geologia e estratigrafia da associacao de rochas do setor centro-norte da peninsula Fildes Ilha Rei George, Shetland do Sul, Antarctica: *Ser. Cient. Inst. Antarct. Chileno* 38, 29–43.

Gao, L., Zhao, Y., Yang, Z., Liu, J., Liu, X., Zhang, S.H., Pei, J., 2018. New paleomagnetic and ⁴⁰Ar/³⁹Ar geochronological results for the South Shetland Islands, West Antarctica, and their tectonic implications. *J. Geophys. Res. Solid Earth* 123, 4–30.

González-Gil, S., Keafer, B.A., Jovine, R.V.M., Aguilera, A., Lu, S., Anderson, D.M., 1998. Detection and quantification of alkaline phosphatase in single cells of phosphorus-starved marine phytoplankton. *Mar. Ecol. Prog. Ser.* 164, 21–35.

Hall, K.J., Walton, D.W.H., D.J., D., Laws, R.M., Pyle, J.A., 1993. Rock weathering, soil development and colonization under a changing climate. Oxford University Press, Oxford, Proceedings of the Royal Society Discussion Meeting on Antarctica and Environmental Change, pp. 69–77.

Havens, S.M., Twiss, R.M., 2007. Evidence for phosphorus, nitrogen, and iron colimitation of phytoplankton communities in Lake Erie. *Limnol. Oceanogr.* 52 (1), 315–328.

Hawkes, D.D., 1961. The Geology of the South Shetland Islands: I. Department of Geology, University of Birmingham, Petrology of King George Island.

Hutchinson, T.C., 1973. Comparative studies of the toxicity of heavy metals to phytoplankton and their synergistic interactions. *Water Qual. Res. J.* 8 (1), 68–90.

Kunz, M., King, M.A., Mills, J.P., Miller, P.E., Fox, A.J., Vaughan, D.G., Marsh, S.H., 2012. Multi-decadal glacier surface lowering in the Antarctic Peninsula. *Geophys. Res. Lett.* 39 (19).

Machado, A., Lima, E.F., Chemale Jr., F., Morata, D., Oteiza, O., Almeida, D.P.M., Figueiredo, A.M.G., Alexandre, F.M., Urrutia, J.L., 2005. Geochemistry constraints of Mesozoic–Cenozoic calc-alkaline magmatism in the South Shetland arc, Antarctica. *J. S. Am. Earth Sci.* 18 (3–4), 407–425.

Malandrino, M., Abollino, O., Buoso, S., Casalino, C.E., Gasparon, M., Giacomino, A., La Gioia, C., Mentasti, E., 2009. Geochemical characterization of Antarctic soils and lacustrine sediments from Terra Nova Bay. *Microchem. J.* 92, 21–31.

Na, G., Liu, C., Wang, Z., Ge, L., Ma, X., Yao, Z., 2011. Distribution and characteristic of PAHs in snow of Fildes Peninsula. *J. Environ. Sci.* 23 (9), 1445–1451.

Pankhurst, R.J., Smellie, J.L., 1983. K-Ar geochronology of the South Shetland Islands, Lesser Antarctica: apparent lateral migration of Jurassic to Quaternary island arc volcanism. *Earth Planet. Sci. Lett.* 66, 214–222.

Perendez, M., Carrasco, M.A., 2003. Elemental composition of surface waters in the Antarctic Peninsula and interactions with the environment. *Environ. Geochem. Health* 25 (3), 347–363.

Prénder, M., Carrasco, A.M., 2003. Elemental composition of surface waters in the Antarctic Peninsula and interactions with the environment. *Environ. Geochem. Health* 25 (3), 347–363.

Priscu, J.C., 1995. Phytoplankton nutrient deficiency in lakes of the McMurdo dry valleys, Antarctica. *Freshw. Biol.* 34 (2), 215–227.

Qayle, W.C., Peck, L.S., Peat, H., Ellis-Evans, J.C., Harrigan, P.R., 2002. Extreme responses to climate change in Antarctic Lakes. *Science* 295, 645.

Rai, L.C., Gaur, J.P., Kumar, H.D., 1981. Phycology and heavy-metal pollution. *Biol. Rev.* 56 (2), 99–151.

Raiswell, R., 1984. Chemical models of solute acquisition in glacial melt waters. *J. Glaciol.* 30 (104), 49–57.

Rintoul, S.R., Chown, S.L., Decontor, M., England, M.H., Fricker, H.A., Masson-Delmotte, V., Naish, T.R., Siebert, M.J., Xavier, 2018. Choosing the future of Antarctica. *Nat. Perspect.* 558, 233–241.

Schmid, T., Lopez-Martínez, J., Guillaso, S., Serrano, E., D'Hondt, O., Koch, M., Nieto, A., O'Neill, T., Mink, S., Duran, J.J., Maestro, A., 2017. Geomorphological mapping of ice-free areas using polarimetric RADARSAT-2 data on Fildes Peninsula and Ardley Island, Antarctica. *Geomorphology* 293 (Part B), 448–459.

Schofield, O., Ducklow, H.W., Martinson, D.G., Meredith, M.P., Moline, M.A., Fraser, W. R., 2010. How do polar marine ecosystems respond to rapid climate change? *Science* 328 (5985), 1520–1523.

Shatova, O., Wing, S.R., Gault-Ringold, M., Wing, L., Hoffmann, L.J., 2016. Seabird guano enhances phytoplankton production in the Southern Ocean. *J. Exp. Mar. Biol. Ecol.* 483, 74–87.

Shatova, O.A., Wing, S.R., Hoffmann, L.J., Wing, L.C., Gault-Ringold, M., 2017. Phytoplankton community structure is influenced by seabird guano enrichment in the Southern Ocean. *Estuar. Coast. Shelf Sci.* 191, 125–135.

- Skidmore, M., Tranter, M., Tulaczyk, S., Lanoil, B., 2010. Hydrochemistry of ice streambeds—evaporitic or microbial effects? *Hydrol. Process.* 24 (4), 517–523.
- Smellie, J.L., Pankhurst, R., Thomson, M.R.A., Davies, R.E.S., 1984. The geology of the South Shetland Islands: VI. Stratigraphy, geo-chemistry and evolution: *British Antarctic Survey* 87, 1–85.
- Soliani, E., Kawashita, K., Fensterseifer, H., Hansen, M.A., Troian, F., 1988. K-Ar ages of the Winkel Point Formation (Fildes Peninsula Group) and associated intrusions, King George Island, Antarctica: *Ser. Cient. INACH* 38, 133–139.
- Sommaruga, R., 2015. When glaciers and ice sheets melt: consequences for planktonic organisms. *J. Plankton Res.* 37 (3), 509–518.
- Spencer, D.F., Greene, R.W., 1981. Effects of nickel on seven species of freshwater algae: *Environmental Pollution Series A. Ecol. Biol.* 25 (4), 241–247.
- Sun, L., Xie, Z., 2001. Changes in lead concentration in Antarctic penguin droppings during the past 3,000 years. *Environ. Geol.* 40, 1205–1208.
- Sunda, W.G., Huntsman, S.A., 1983. Effect of competitive interactions between manganese and copper on cellular manganese and growth in estuarine and oceanic species of the diatom *Thalassiosira*. *Limnol. Oceanogr.* 28, 924–934.
- Sunda, W.G., Huntsman, S.A., 1995. Iron uptake and growth limitation in oceanic and coastal phytoplankton. *Mar. Chem.* 50, 189–206.
- Thalasso, F., Sepulveda-Jauregui, A., Cabrol, L., Lavergne, C., Olgun, N., Martinez-Cruz, K., Aguilar-Muñoz, P., Calle, N., Mansilla, A., Astorga-España, M.S., 2022. Methane and carbon dioxide cycles in lakes of the King George Island, maritime Antarctica. *Sci. Total Environ.* v, 848.
- Turner, J., Colwell, S.R., Marshall, G.J., Lachlan-Cope, T.A., Carleton, A.M., Jones, P.D., Lagun, V., Reid, P.A., Iagovkina, S., 2005. Antarctic climate change during the last 50 years. *Int. J. Climatol.* 25 (3), 279–294.
- Utermöhl, H., 1958. Zur Vervollkommnung der quantitativen Phytoplankton-Methodik. *Mitt. int. Verein. theor. angew. Limnology* 9, 1–38.
- West, W.E., Creamer, K.P., Jones, S.E., 2015. Productivity and depth regulate lake contributions to atmospheric methane. *Limnol. Oceanogr.* v <https://doi.org/10.1002/lno.10247>.
- Wetzel, R.B., 2001. The Phosphorus Cycle, *Limnology Lake and River Ecosystems*. San Diego, Elsevier Academic Press, Volume Third Edition, pp. 239–288.
- Wolff-Boenisch, D., Gislason, S.R., Oelkers, E.H., Putnis, Christine V., 2004. The dissolution rates of natural glasses as a function of their composition at pH 4 and 10.6, and temperatures from 25 to 74°C. *Geochim. Cosmochim. Acta* 68 (23), 4843–4858.
- Yogui, G.T., Sericano, J.L., 2008. Polybrominated diphenyl ether flame retardants in lichens and mosses from King George Island, maritime Antarctica. *Chemosphere* 73, 1589–1593.

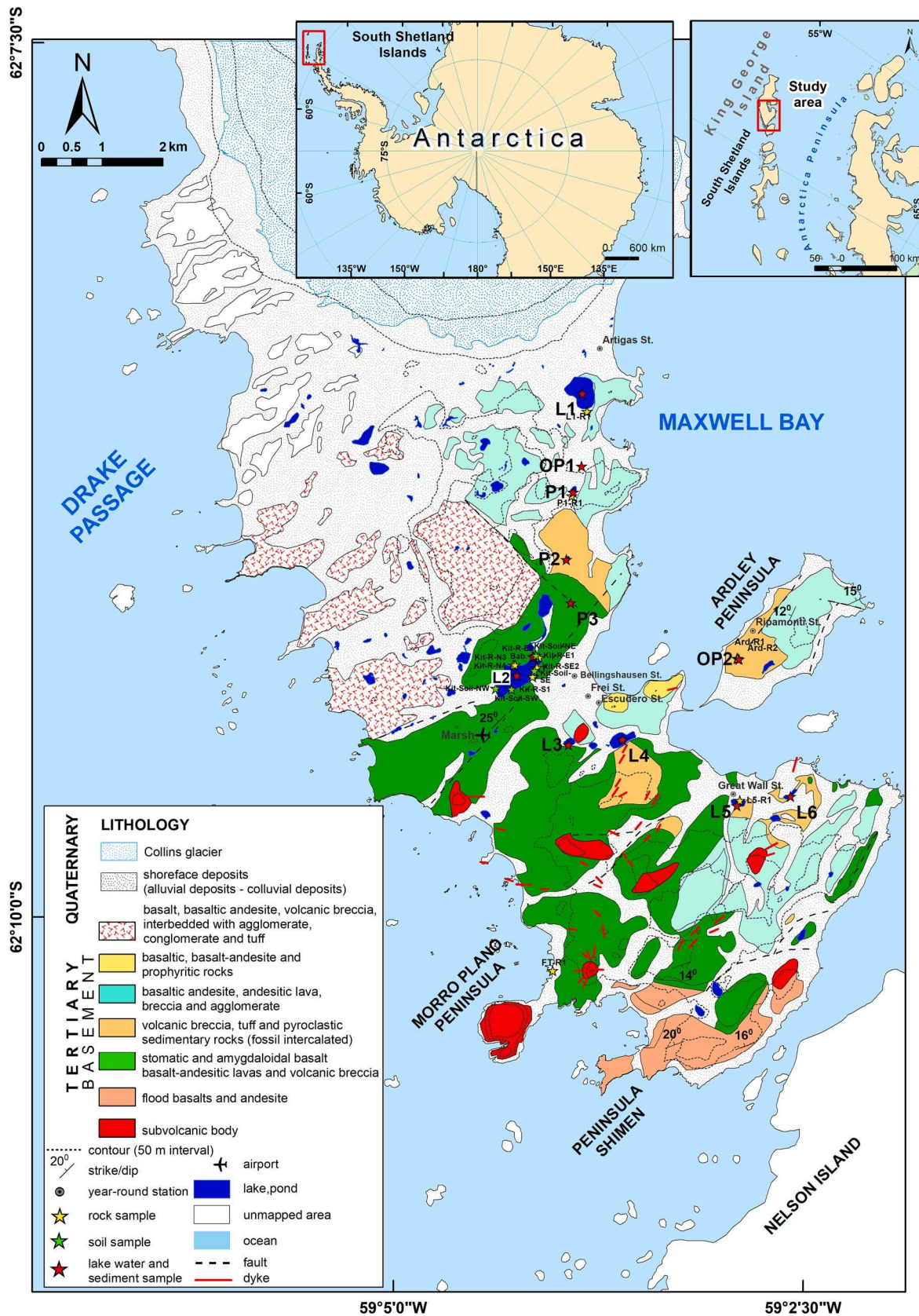


Fig. 1. Locations of water, sediment, soil, and rock samples from the studied lakes, ponds, and streams in the Fildes and Ardley Peninsulas in King George Island, South Shetland Islands, maritime Antarctica. The geologic map was based on Gao et al., 2018, Machado et al., 2005. Hydrographic elements were digitized by using the 1:10.000 scaled printed topography map provided by the Instituto Geografico Militar-IGM, Santiago, Chile, 2012.



Fig. 2. Field photographs of the studied lakes in King George Langer Lake (L4), (c) L3, (d) OP2 and (f) West Lake (L5), (g) an example outcrop of rock showing frost weathering cracks located southeast of Kitiesh lake, (h, i) photographs of studied rock samples from Kitiesh Lake region and (j) a rock sample samples in the littoral zone of OP2 from Ardley Island with green alteration surface and black radial surface encrustations.

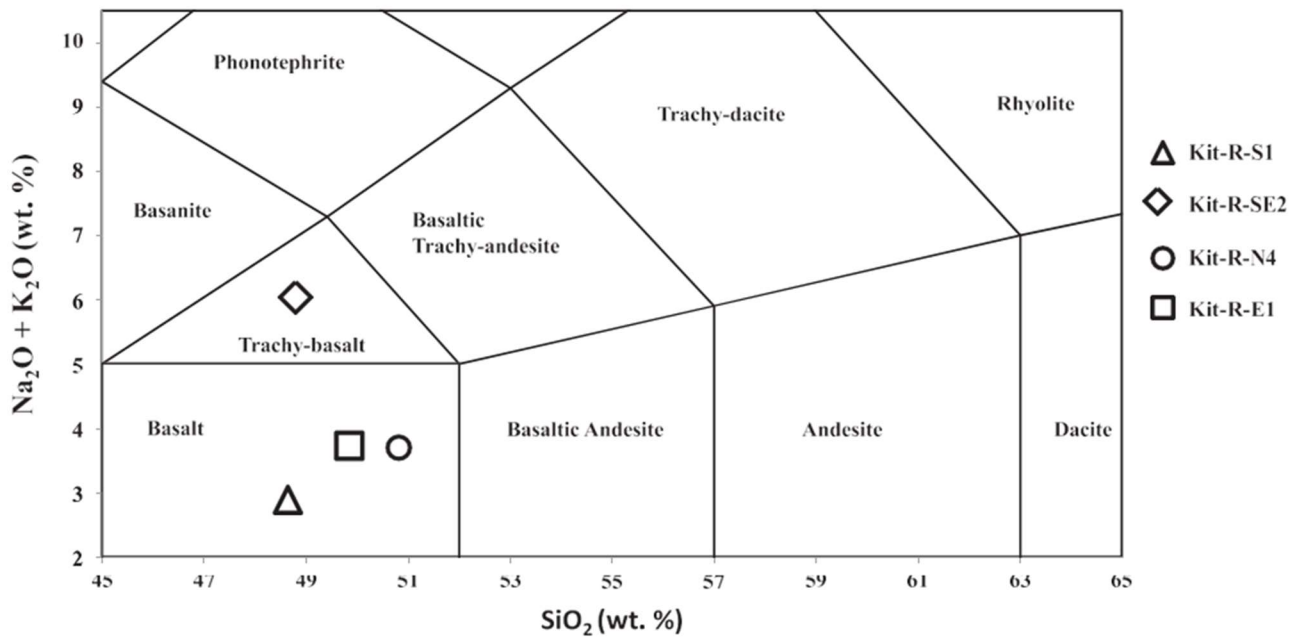
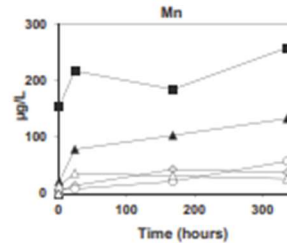
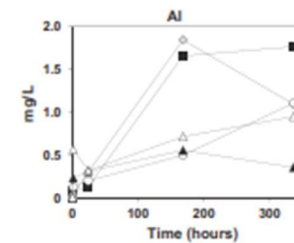
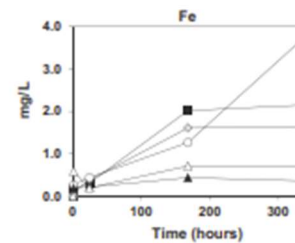
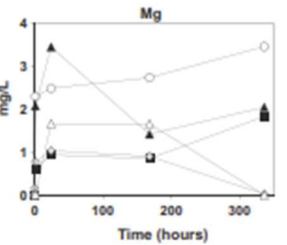
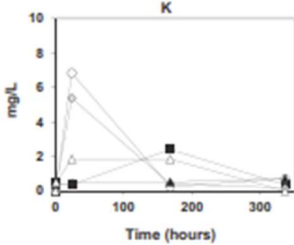
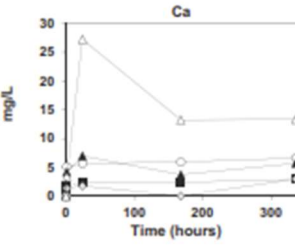
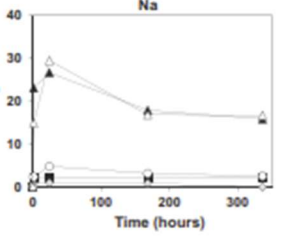
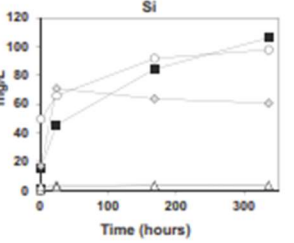
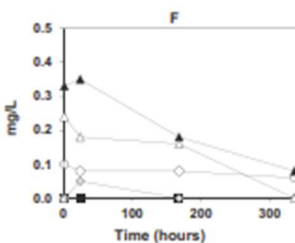
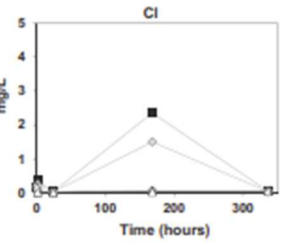
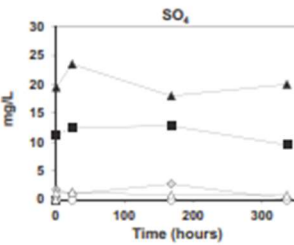
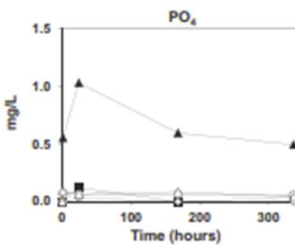
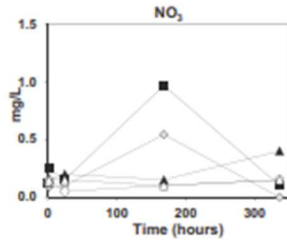
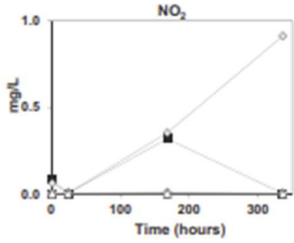
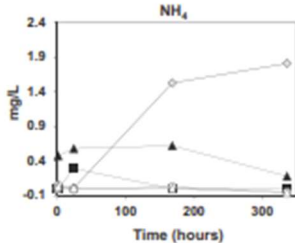
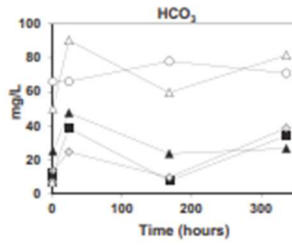
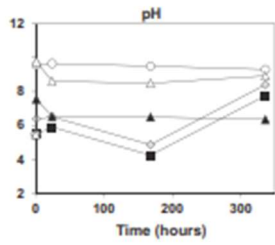
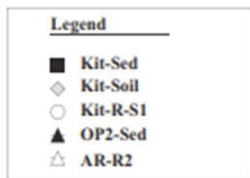


Fig. 3. TAS Diagram showing the types of volcanic rock samples based on the Total Alkali (Na₂O + K₂O %) and silicate (SiO₂%) concentrations.



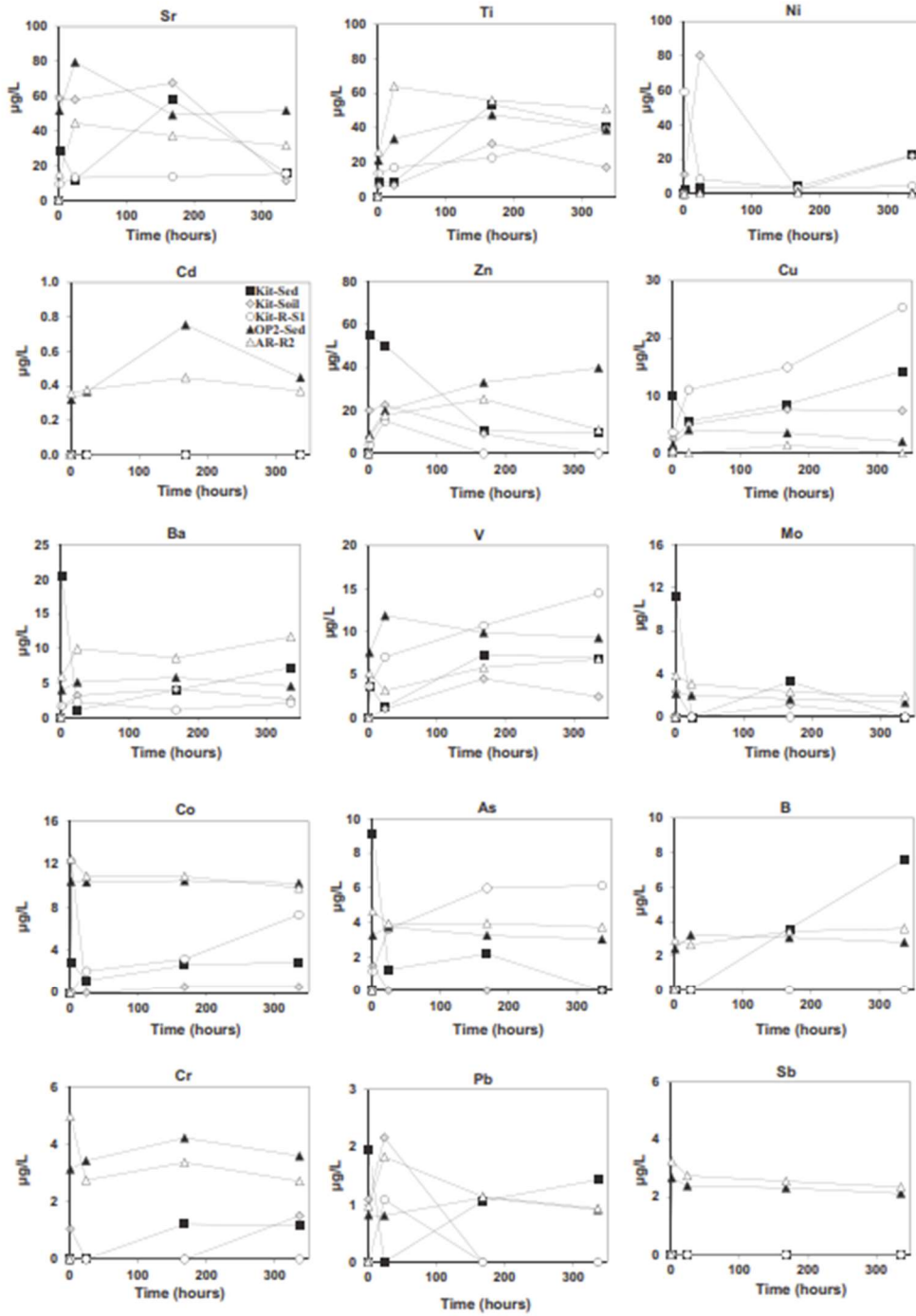


Fig. 4. Results of the leaching experiments in ultra-pure water. $T_0 = 0$, $T_1 = 1$ -h, $T_2 = 2$ -h, $T_3 = 168$ -h (1 week), $T_4 = 336$ -h (2 weeks).